



Published in final edited form as:

J Leukoc Biol. 2023 July 01; 114(1): 1–20. doi:10.1093/jleuko/qiad028.

Phagocytosis via complement receptor 3 enables microbes to evade killing by neutrophils

Asya Smirnov^{*¶}, Kylene P. Daily^{*¶}, Mary C. Gray^{*}, Stephanie A. Ragland^{*¶}, Lacie M. Werner^{*}, M. Brittany Johnson^{*¶}, Joshua C. Eby[†], Erik L. Hewlett[†], Ronald P. Taylor[‡], Alison K. Criss^{*§}

^{*}Department of Microbiology, Immunology, and Cancer Biology

[†]Division of Infectious Diseases and International Health, Department of Medicine

[‡]Department of Biochemistry and Molecular Genetics, University of Virginia School of Medicine

Abstract

Complement receptor 3 (CR3; CD11b/CD18; $\alpha_m\beta_2$ integrin) is a conserved phagocytic receptor. The active conformation of CR3 binds the iC3b fragment of complement C3 as well as many host and microbial ligands, leading to actin-dependent phagocytosis. There are conflicting reports about how CR3 engagement affects the fate of phagocytosed substrates. Using imaging flow cytometry, we confirmed that binding and internalization of iC3b-opsonized polystyrene beads by primary human neutrophils was CR3-dependent. iC3b-opsonized beads did not stimulate neutrophil reactive oxygen species (ROS), and most beads were found in primary granule-negative phagosomes. Similarly, *Neisseria gonorrhoeae* (Ngo) that does not express phase-variable Opa proteins suppresses neutrophil ROS and delays phagolysosome formation. Here, binding and internalization of Opa-deleted (opa) Ngo by adherent human neutrophils was inhibited using blocking antibodies against CR3 and by adding neutrophil inhibitory factor, which targets the CD11b I-domain. No detectable C3 was deposited on Ngo in the presence of neutrophils alone. Conversely, overexpressing CD11b in HL-60 promyelocytes enhanced opa Ngo phagocytosis, which required CD11b I domain. Phagocytosis of Ngo was also inhibited in mouse neutrophils that were CD11b-deficient or treated with anti-CD11b. Phorbol ester treatment upregulated surface CR3 on neutrophils in suspension, enabling CR3-dependent phagocytosis of opa Ngo. Neutrophils exposed to opa Ngo had limited phosphorylation of Erk1/2, p38, and JNK. Neutrophil phagocytosis of unopsonized *Mycobacterium smegmatis*, which also resides in immature phagosomes, was CR3-dependent and did not elicit ROS. We suggest that CR3-

[§]Correspondence: Alison K. Criss, Department of Microbiology, Immunology, and Cancer Biology, Box 800734, University of Virginia School of Medicine, Charlottesville, VA 22908-0734. Phone: (434) 243-3561; Fax: (434) 982-1071; akc2r@virginia.edu.

[¶]Present affiliations: AS, Department of Molecular Microbiology, Washington University School of Medicine; KPD, Department of Microbial Infection and Immunity, College of Medicine, The Ohio State University; SAR, Division of Gastroenterology, Boston Children's Hospital; MBJ, Department of Biological Sciences, University of North Carolina-Charlotte

AUTHORSHIP

Conceptualization: AS, ELH, RPT, AKC; Formal analysis: AS, KPD, MCG, SAR, LMW, MBJ; Funding Acquisition: AKC; Investigation: AS, KPD, MCG, SAR, MBJ; Methodology: AS, SAR, JCE; Project Administration: AKC; Resources: JCE, ELH, RPT; Supervision: AKC; Validation: MCG, LMW; Visualization: AKC, AS, MCG, SAR, LMW, MBJ; Writing-Original Draft: AS, AKC; Writing-Review and Editing: AS, KPD, MCG, SAR, LMW, MBJ, JCE, ELH, RPT, AKC.

CONFLICT OF INTEREST DISCLOSURE

The authors declare no conflicts of interest.

mediated phagocytosis is a silent mode of entry into neutrophils, which is appropriated by diverse pathogens to subvert phagocytic killing.

Summary Sentence:

In neutrophils, complement receptor 3 mediates phagocytosis of iC3b-opsonized beads and unopsonized *Neisseria gonorrhoeae* and *Mycobacterium smegmatis* without full oxidant release, degranulation, or proinflammatory signaling.

Keywords

Neisseria gonorrhoeae ; neutrophil; phagocytosis; integrin; phagocytosis; CR3; complement; *Mycobacterium smegmatis*

INTRODUCTION

As first responders to infection and sterile inflammation, neutrophils have a dynamic capacity for phagocytosis of both foreign and host material [1]. How this material is recognized by host receptors influences the extent of phagocytosis and the subsequent fate of the material. Phagocytosis of substrates can proceed through opsonization by soluble components such as antibody and complement, and can also be independent of opsonization by interaction with neutrophil receptors that directly recognize the material. After phagocytosis, the nascent phagosome fuses with cytoplasmic granules to form a mature phagosolysosome, and assembly of NADPH oxidase on the phagosome generates antimicrobial reactive oxygen species (ROS), a hallmark of neutrophil activation [2, 3]. Fusion of secondary/specific granules to phagosomes or to the plasma membrane releases pro-forms of cathelicidin antimicrobial peptides, the nutritional immunity protein lactoferrin, and the cytochrome_{b558} component of NADPH oxidase, while primary/azurophilic granule fusion releases serine proteases such as neutrophil elastase, α -defensins, and myeloperoxidase [2]. The concerted action of these factors in the phagolysosome mediates killing of microbes and digestion of the phagocytosed material [1]. Granule mobilization, ROS production, and kinase cascades that lead to production and release of proinflammatory cytokines are modulated by the signals emanating from phagocytic receptors, as well as through co-receptors that recognize the material but are not themselves phagocytic [4].

Neutrophils are characterized by the abundant surface expression of complement receptor 3 (CR3; $\alpha_m\beta_2$; CD11b/CD18). CR3 is an integrin heterodimer that is critical for the chemotaxis and phagocytic activity of neutrophils and macrophages [5]. On naïve phagocytes CR3 is in an inactive conformation. Complex inside-out and outside-in signals place CR3 in an active, ligand binding-proficient state, with the CD18 cytoplasmic tail interacting with the F-actin cytoskeleton via talin, vinculin, and kindlin (reviewed in [6]). Although the canonical ligand for CR3 is the complement fragment iC3b, CR3 binds a diverse array of ligands that are both host- and microbial-derived, including extracellular matrix proteins, the cathelicidin LL-37, fungal β -glucan, and bacterial toxins, lipopolysaccharide, and adhesins [7–15]. Binding to iC3b and many other ligands is predominantly mediated by the I-domain, an extension that is found in leukocyte CD11

proteins relative to other α integrins [5]. Overlapping with, but distinct from the CD11b I-domain is the metal ion-dependent adhesion site (MIDAS) that also promotes ligand binding [5]. While the ability of CR3 to facilitate phagocytosis is well accepted, there are differing reports concerning whether CR3 engagement leads to phagolysosome formation and ROS production by neutrophils (reviewed in [16]).

Given the central role of neutrophils in recognition of and response to microbial challenge, it is not surprising that some pathogens make use of mechanisms to resist phagocytic killing by neutrophils. These mechanisms include evasion of opsonophagocytosis by preventing antibody or complement deposition, expression of antiphagocytic surface components like capsules, use of toxins or bacterially-injected proteins to block phagosome-granule fusion, and resistance to neutrophil antimicrobial components (reviewed in [17]). One pathogen that evades neutrophil-mediated clearance is the bacterium *Neisseria gonorrhoeae* (Ngo), which causes the sexually transmitted disease gonorrhea [18]. In symptomatic gonorrhea, neutrophils are recruited in abundance to mucosal sites of infection. However, viable, infectious Ngo are recovered from the resulting neutrophil-rich purulent exudates, indicating Ngo has strategies to resist clearance by neutrophils [19].

The major determinant of the fate of Ngo inside neutrophils is how it is phagocytosed, which is influenced by the physiological state of the neutrophil [20]. The predominant driver of nonopsonic interaction of Ngo with neutrophils is the family of opacity-associated (Opa) surface-exposed proteins [21–23]. Each of the 10–14 *opa* genes in Ngo is independently phase-variable, conferring an extensive capacity for surface variation in the bacterial population. Most Opa proteins bind human carcinoembryonic antigen-related cell adhesion molecules (CEACAMs), of which CEACAMs 1, 3, and 6 are expressed by neutrophils [24]. Opa-expressing (“Opa+”) Ngo that bind the granulocyte-restricted, immunotyrosine activation motif (ITAM)-bearing CEACAM3 is rapidly phagocytosed into mature phagolysosomes and stimulates reactive oxygen species (ROS) production [25–27]. In contrast, unopsonized Opa-negative Ngo is not phagocytosed by neutrophils in suspension and does not stimulate ROS production [20, 28, 29]. We have reported that adherent, interleukin-8 treated human neutrophils can phagocytose Opa-negative Ngo, although they do so more slowly than when they internalize Opa+ bacteria. Moreover, their phagosomes exhibit delayed fusion with primary granules, enabling intracellular survival [30–32]. IgG-opsonized Ngo phenocopies CEACAM3-binding bacteria, while serum-opsonized bacteria do not stimulate ROS production or phagolysosome formation [31]. The mechanism by which adherent but not suspension neutrophils phagocytose unopsonized, Opa-negative Ngo has not been identified.

In this study we define CR3-mediated phagocytosis as a mechanism of “silent entry” into neutrophils, which does not trigger ROS production, early phagolysosome formation, or intracellular proinflammatory signaling cascades. These outcomes are shown for three unrelated substrates: iC3b-opsonized beads, *Mycobacterium smegmatis*, and Opa-negative Ngo, which we found exploits CR3 for phagocytosis by adherent neutrophils. Suspension neutrophils gained the capacity for phagocytosis of Opa-negative Ngo when CR3 was ectopically activated, and overexpression of CD11b enabled phagocytosis of Opa-negative Ngo by HL-60 human promyelocytes. From these results, we posit that neutrophils use CR3

for silent phagocytosis of material with limited cellular activation. This process is exploited by diverse pathogens to survive confrontation with these otherwise antimicrobial cells.

METHODS

Chemicals, reagents, and antibodies.

All chemicals and reagents were from ThermoFisher Scientific unless otherwise noted. Antibody sources and reactivities are provided in Table 1.

Bacterial strains and growth conditions.

This study used the constitutively piliated *opa* (Opaless; *opaA-K*) and isogenic constitutively OpaD-expressing (OpaD+) Ngo of strain background FA1090 [33]. Other strain backgrounds used were piliated, *recA6* FA1090 RM11.2 [34], constitutively piliated derivative of MS11 VD300 [35], and piliated 1291 (gift of M. Apicella, Univ. of Iowa). Phenotypically translucent colonies from these three Opa-variable strain backgrounds were used for experiments. The absence of Opa expression in these derivatives was confirmed by immunoblotting with the 4B12 anti-Opa antibody [36].

Ngo was grown on solid GCB media containing Kellogg's supplement I and II [37] for 16–18 hr at 37°C, 5% CO₂. Viable, exponential-phase predominantly piliated (except the *pilE* and *pilQ* mutants) bacteria were grown in rich liquid medium with three sequential dilutions [38]. For opsonization, Ngo was incubated with gentle rotation in 10% pooled normal human serum (Sigma) for 20 min at 37°C as described previously [32]. Complement deposition on the Ngo surface was visualized by immunofluorescence using a fluorescein-conjugated antibody against human C3.

M. smegmatis strain mc2 155 was from G. Ramakrishnan (Univ. of Virginia), and an mCherry-expressing derivative (mgm1732; generated by transformation of mc2 155 with the pCherry3 mCherry expression plasmid [39, 40]) was from C. Stallings (Washington Univ.). Bacteria were maintained on LB agar with 50% glycerol and 40% dextrose (with 50 µg ml⁻¹ hygromycin for mgm1732). For experiments, bacteria were inoculated in LB liquid medium with 50% glycerol, 40% dextrose, and 0.25% Tween 80 (Sigma) (with 50 µg ml⁻¹ hygromycin for mgm1732) and shaken at 150 rpm at 37 °C for 48 hr.

Where indicated, bacteria were labeled with 5 µg ml⁻¹ carboxylfluorescein diacetate succinimidyl ester (CFSE) or Tag-IT Violet™ proliferation and cell tracking dye (Biolegend) in PBS containing 5 mM MgSO₄, at 37°C for 20 min in the dark, then pelleted and washed before use in experiments.

Ngo mutant construction.

***pilE*:** Overlap extension PCR was used to replace most of the *pilE* open reading frame with a PvuII restriction site. Using genomic DNA from FA1090 that is nonvariable for the 1–81–S2 *pilE* sequence and has deletions in *opaB*, *opaE*, *opaG*, and *opaK* [33], the 5' end of *pilE* and flank was amplified with primers PilE-RA 5'-TTGGGCAACCGTTTTATCCG-3' and PilE-FA 5'-

GCCTAATTTGCCTTAGGTGGCAGACAGCTGTTATTGAAGGGTATTCATAAAATTAC

TCC-3', the 3' end of *pilE* and flank was amplified with primers PilE-RB 5'-GGCGTCGTCTTTGGCGA-3' and PilE-FB 5'-GGAGTAATTTTATGAATACCCCTTCAATAACAGCTGTCTGCCACCTAAGGCAAATTA GGC-3' (PvuII site underlined), and the two products were combined for overlap extension PCR using PilE-FA and PilE-RB. The resulting 1.5 kb product was spot transformed into *opa* Ngo [41], and P- colonies were phenotypically selected and streak purified. The presence of the deletion was confirmed by PCR using primers PILRBS and PilE-RA, and Southern blot of XhoI and ClaI-digested genomic DNA with a digoxigenin-labeled *pilE* probe, amplified from the pilated parent.

pilT: The *pilT* gene and flanking sequence from the FA1090 chromosome was amplified by PCR with primers PilT-F 5'-CATTGAGGTCCGCAAGCAGC-3' and PilT-R 5'-GCATCTTTACCCAGCGCGAAAT-3' and cloned into pSMART HC Kan (Lucigen). The cloning mix was transformed into TOP10 *E. coli*, transformants were selected on 50 $\mu\text{g ml}^{-1}$ kanamycin, and the presence of the insert was confirmed by PCR and sequencing (Genewiz). The plasmid was purified from *E. coli* by miniprep (Qiagen), and the internal 504 bp of *pilT* was removed by digestion with AccI (New England Biolabs). The plasmid was religated with T4 DNA ligase (New England Biolabs) and transformed into TOP10 *E. coli*. The presence of the deletion was confirmed by PCR and sequencing. The *pilT* plasmid was spot transformed into *opa* Ngo, and transformants were selected based on the characteristic jagged edge colony morphology of *pilT* mutant Ngo. Transformants were passaged on GCB, and the presence of the deletion was determined by product size following PCR amplification with PilT-F 5'-TTACCGACTTACTCGCCTTCG-3' and PilT-R 5'-CGATTGCAGCGATTGGTCC-3' and confirmed by DNA sequencing.

pilQ: *opa* Ngo was spot transformed with a plasmid carrying the *pilQ* gene interrupted by a chloramphenicol resistance cassette (from H. Seifert, Northwestern Univ.) [42]. Transformants were selected on 0.5 $\mu\text{g ml}^{-1}$ chloramphenicol and passaged sequentially three times on chloramphenicol-GCB. The presence of *pilQ::cat* was confirmed by P-colony morphology, PCR using pilQ-F 5'-CGCAACCGCCGCCTTTCA-3' and pilQ-R 5'-CAGCCTGCGCTATTGATGC-3', and Southern blot using a *pilQ* digoxigenin-labeled probe.

pgIA, pgID: Genomic DNA from *pgIA::kan* and *pgID::kan* in strain background 1291 (from J. Edwards, Nationwide Children's) was transformed into *opa* Ngo, followed by two more rounds of backcrossing from confirmed transformants. In all cases, transformants were selected on GCB containing 50 $\mu\text{g mL}^{-1}$ kanamycin, and the presence of the mutated gene confirmed by PCR and sequencing (*pgIA*: *pgIA*-F 5'-ACAACAGTCGCATCCAGCAT-3' and *pgIA*-R 5'-CGGGGATTCCAAGGTTTCGAT-3'; *pgID*: *pgID*-F 5'-ATCTGGAAACCCTGATCGCC-3' and *pgID*-R 5'-TTCGCATACCCAAAGCAGGT-3').

Human neutrophil purification.

Peripheral venous blood was drawn from healthy human subjects with informed consent, in accordance with a protocol approved by the University of Virginia Institutional Review

Board for Health Sciences Research (#13909). Neutrophils were purified by dextran sedimentation followed by Ficoll separation and hypotonic lysis of residual erythrocytes as in [38]. Neutrophil content in suspension was >90% as monitored by phase-contrast microscopy and confirmed by flow cytometry (CD11b⁺/CD14⁻/CD49d^{low}/CD16^{high}). All replicate experiments were conducted using neutrophils from different subjects.

Bacterial association with and internalization by adherent primary human neutrophils.

Neutrophils were suspended in RPMI (Cytiva) + 10% heat-inactivated fetal bovine serum (HyClone) (hereafter referred to as “infection medium”) containing 10 nM human IL-8 (R&D Systems) and left to adhere to tissue culture-treated plastic coverslips (Sarstedt) for 30 min. Neutrophils were treated with blocking antibodies or matched isotype control (20 µg ml⁻¹; see Table 1), or recombinant *A. caninum* NIF protein (R&D Systems; 0.5 µg ml⁻¹) for 20 min. Fluorescently labeled Ngo was then added to neutrophils by centrifugation at 400 xg for 4 min at 12 °C. The supernatant was discarded to remove unbound bacteria, pre-warmed infection medium was added, and the cells and bacteria were coincubated for 1 hr at 37 °C and 5% CO₂ [38]. Cells were fixed with 2% paraformaldehyde (PFA) (Electron Microscopy Sciences) for 10 min on ice, collected into microfuge tubes using a cell scraper, and washed (600 x g, 4 min DPBSG washes x 3). Non-specific antibody binding was blocked with 10% normal goat serum for 10 min followed by staining with anti-Ngo antibody coupled to DyLight™ 650 (ThermoFisher).

Cells were analyzed by imaging flow cytometry using ImageStream^X Mark II operated by INSPIRE software (Luminex). Bacterial association with neutrophils was measured using IDEAS 6.2 Software (Luminex) as previously described [43]. Briefly, the percent of neutrophils with associated Ngo was calculated as the percent of CFSE⁺ or Tag-IT Violet⁺ cells, and the percent of neutrophils with internalized Ngo was calculated using spot count and a step gate function as the percent of cells with 1 CFSE⁺ or Tag-IT Violet⁺ only bacterium. For *M. smegmatis*-infected neutrophils, extracellular bacteria were not identified by differential fluorescence. Instead, intracellular bacteria were defined as those whose entirety was within a mask that was eroded by 4 pixels from the neutrophil periphery, as marked by staining for surface CD11b. The single cell population was identified as the population of cells with medium area and medium to high aspect ratio. Cell morphology was visually verified within the gate boundaries.

Phagocytosis of opsonized sheep red blood cells by adherent primary human neutrophils.

Sheep red blood cells (sRBCs) (MP Biomedicals) were opsonized with iC3b in gelatin veronal buffer, using anti-sRBC IgM and C5-deficient human serum as in [44]. Complement deposition on sRBCs was confirmed by using fluorescein-conjugated rabbit anti-human C3 antibody (10 µg mL⁻¹, 30 min incubation at 37 °C). Adherent, IL-8 treated primary human neutrophils, incubated in infection medium, were exposed to 150 ng mL⁻¹ phorbol myristate acetate (PMA; Sigma) for 5 min at 37 °C to activate CR3. Neutrophils were incubated with blocking antibodies or isotype control (20 mg ml⁻¹, 20 min), then exposed to 10⁶ opsonized sRBCs in infection medium at 37 °C for 10 min. Plates were centrifuged at 600 x g for 4 min at 12°C and then put on ice to stop phagocytosis. Media was removed, extracellular sRBCs were lysed with endotoxin free water (ICUMedical) for 1 min, and neutrophils were

incubated in ice cold methanol for 10 min. Cells were washed once with water and mounted on slides for imaging. The phagocytic index is reported as the number of intracellular opsonized sRBCs per 100 neutrophils.

Ngo infection of human neutrophils in suspension.

Primary human neutrophils (3×10^6) were suspended in Dulbecco's PBS without calcium or magnesium (Gibco) with 0.1% glucose (DPBSG-). Neutrophils were left untreated or exposed to 200 nM PMA for 10 min. After treatment with blocking antibodies or isotype control (20 mg ml⁻¹), unlabeled or CFSE-labeled Ngo was added to the neutrophils at multiplicity of infection = 1 unless otherwise indicated and incubated at 37 °C for 1 hr with slow rotation. Cells were stained with Zombie Violet viability dye (BioLegend), fixed with 1% paraformaldehyde (PFA) for 10 min, and analyzed by imaging flow cytometry as above. Surface presentation of total (ICRF44) and active (CBRM1/5) CD11b was analyzed by flow cytometry.

Ngo infection of HL-60 cells.

HL-60 cells expressing either empty vector, human CD11b full length, or CD11b lacking I-domain (from V. Torres, NYU; [8]) were incubated with CFSE+ Ngo at the indicated MOI at 37°C for 1 hr, followed by anti-Ngo antibody coupled to DyLight™ 650. The percent of CFSE+ HL-60 cells with intracellular Ngo (1 CFSE only spot) was measured by imaging flow cytometry using a step gate as for primary human neutrophils.

***N. gonorrhoeae* association with and internalization by mouse neutrophils.**

Experiments with mice were approved by the Animal Care and Use Committee at the University of Virginia and supported exclusively by internal funds at the University of Virginia. The tibiae, femurs, and vertebrae were harvested from 4–8 week old, male WT (#000664) and *cd11b*^{-/-} (#003991, B6.129S4-*Itgam*^{tm1myd/J}) C57BL/6J mice (Jackson Laboratories). Male mice were used as they were available at the time these experiments were initiated; there are no reports to suggest that CR3 on neutrophils from male and female mice would respond differently. Bone marrow was extracted by mortar and pestle, and neutrophils were purified using an antibody-based negative selection kit (Stem Cell Technologies). Purified neutrophils were >84% viable (using Zombie Violet, Biolegend) and >80% Ly6G^{hi}CD11b^{hi}. Neutrophils purified from *CD11b*^{-/-} mice were confirmed to be Ly6G^{hi}CD11b^{neg} by flow cytometry.

Plastic tissue culture coverslips were coated with normal mouse serum (50% diluted in DPBS with CaCl₂ and MgCl₂) (Sigma) for 1 hr at 37°C with 5% CO₂, and residual serum was removed by aspiration. Mouse neutrophils were resuspended in infection medium and allowed to adhere onto the serum-treated coverslips for 1 hr at 37°C with 5% CO₂. Neutrophils were treated with M170 anti-CD11b antibody or isotype control, or left untreated, then exposed to CFSE-labeled Ngo. Association and internalization of Ngo by mouse neutrophils was determined as for adherent primary human neutrophils.

Bead opsonization.

Fluoresbrite® Brilliant Blue Carboxylate Microspheres (1.0 µm diameter, Polyscience) were incubated with iC3b (Complement Technology) at 37 °C for 1 hr. Under these conditions, iC3b is not covalently linked to the beads. Beads were washed and mixed with 3E7 anti-human iC3b antibody [45] (IgG+iC3b opsonized) or an equal volume of PBS (iC3b opsonized) and incubated at 37 °C for 1 hr. Imaging flow cytometry was used to confirm deposition of iC3b ± IgG using FITC anti-C3 and AlexaFluor 647-coupled anti-mouse IgG as in [46].

Phagosome maturation.

Adherent primary human neutrophils were treated with 150 ng mL⁻¹ PMA as for experiments with sRBC, then incubated with iC3b- or iC3b + IgG-opsonized beads at a ratio of 1 bead:neutrophil. At the indicated times, the medium was aspirated and neutrophils were fixed in 2% PFA. Neutrophils were stained with FITC-labeled anti-C3 without permeabilization to identify extracellular beads, then permeabilized with ice-cold 1:1 acetone:methanol for 2 min and incubated with rabbit anti-human lactoferrin followed by goat anti-rabbit AlexaFluor 555, or AlexaFluor 555-coupled mouse anti-neutrophil elastase (primary granules).

For *M. smegmatis*, neutrophils were incubated with mCherry-expressing bacteria at MOI = 5 for 1 hr. Neutrophils were fixed in 4% PFA, then permeabilized and stained for lactoferrin or elastase as above. OpaD+ and opa Ngo were used as positive and negative controls, respectively, for elastase-dependent phagosome maturity.

Intracellular bacteria or beads were considered to be in a positive phagosome if surrounded by > 50% of a ring of fluorescence for the granule protein of interest. 100–200 phagosomes were analyzed per condition. AS and two blinded observers independently quantified the micrographs, and percent positive phagosomes are reported as the average reported by the three observers.

Talin immunofluorescence.

Adherent, IL-8 treated primary human neutrophils were exposed to CFSE-labeled opa Ngo as above. After 10 min or 60 min, cells were fixed in 4% PFA. Extracellular Ngo was identified using AlexaFluor 647-coupled anti-Ngo antibody without permeabilization. Cells were re-fixed in PFA, permeabilized with 0.1% saponin in PBS with 10% normal goat serum, and incubated with an Alexa Fluor 555-coupled antibody against talin.

Complement C3 production by human and mouse neutrophils.

Adherent neutrophils (not IL-8 treated) were exposed to 5 µg mL⁻¹ cytochalasin B (Sigma) for 20 min followed by 1 µM fMLF (Sigma) for 10 min to stimulate degranulation, or they were instead treated with the DMSO control. Supernatants were passed through a 0.2 µm filter. opa Ngo (2 x 10⁸ CFU) was incubated with 1 mL neutrophil supernatant for 20 min at 37° C, pelleted, and washed. Ngo was fixed and processed for imaging flow cytometry, or resuspended in 1x SDS sample buffer for Western blot, in both cases using goat anti-human complement C3 antibody to detect C3 deposition on Ngo. Imaging flow cytometry data

acquisition and analysis were performed as previously described for N-CEACAM binding to Ngo [46]. Ngo incubated with 10% pooled human serum (Complement Technologies) for 20 min at 37 °C was used as positive control, and Ngo incubated with 10% C3-deficient human serum (Complement Technologies), 10% heat inactivated normal human serum (Sigma), or 10% FBS in RPMI served as negative controls.

Neutrophil phosphoproteins.

Human neutrophils (1×10^7) were suspended in DPBS containing 0.1% dextrose, 1.25 mM CaCl_2 , 0.5 mM MgCl_2 , 0.4 mM MgSO_4 and incubated with unopsonized opa or OpaD+ Ngo for indicated times at 37 °C. Neutrophils were pelleted by centrifugation at $1000 \times g$ at 4°C for 10 min, then resuspended and lysed in 1x SDS sample buffer containing 20 µg/ml aprotinin (ICN), 1 mM PMSF, 20 µg ml⁻¹ leupeptin, 20 µg ml⁻¹ pepstatin, 40 mM β-glycerophosphate, 10 µM calyculin A, 5 mM NaF, 1 mM Na_3VO_4 , and 1 mM EDTA. Lysates were separated by SDS-PAGE and analyzed by immunoblot using antibodies for total and phosphorylated AKT, p38, and Erk1/2, followed by goat anti-mouse IgG (H+L) DyLight™ 800 and goat anti-rabbit (H+L) Alex Fluor 680. Bands were quantitated using near-infrared fluorescence detection with the Odyssey imaging system (LI-COR Biosciences). The ratio of phospho-protein to total protein at each time point for each condition was normalized to the ratio for the uninfected neutrophils at 10 min, which was set to a value of 1.

Neutrophil degranulation.

The surface presentation of CD11a, CD11b (total and active), CD11c, CD63, and CD66b was measured by flow cytometry as in [35]. The gate for CD63 or CD66b positivity was set based on the isotype control. Results are reported as geometric mean fluorescence intensity for n=6 biological replicates.

Reactive oxygen species production.

Human neutrophils were exposed to opsonized beads (see above) at a ratio of 100 beads:neutrophil, or exposed to bacteria at MOI = 100. Production of reactive oxygen species over time was measured by luminol-dependent chemiluminescence as in [38].

opa and OpaD+ Ngo served as negative and positive controls, respectively. Results are representative of at least 3 independently conducted experiments.

Fluorescence microscopy.

Slides were imaged on a Nikon Eclipse E800 UV/visible fluorescence microscope with Hamamatsu Orca-ER digital camera using Openlab (Improvision) or NIS Elements (Nikon) software. Images were exported and processed using Adobe Photoshop CC2019.

Statistics.

Comparisons were made with Student's *t* test, or one- or two-way ANOVA with appropriate multiple comparisons test as indicated in each figure legend, using Graphpad Prism version 9.2.0 for Windows, GraphPad Software, San Diego, California USA, www.graphpad.com. In experiments with human neutrophils, statistical tests took into account the potential

variability of human subjects' cells by using paired tests. $P < 0.05$ was considered significant, and specific P values are indicated in each legend.

RESULTS

CR3-dependent phagocytosis elicits weak oxidant production and primary granule mobilization in human neutrophils.

The canonical ligand for CR3 is the iC3b fragment of complement. To define the consequences of CR3 engagement on neutrophil functionality, we exposed fluorescent carboxylate beads that were opsonized with iC3b to adherent, IL-8 treated primary human neutrophils, to mimic the tissue-migrated state of neutrophils responding to infection or injury. First, we confirmed that phagocytosis of iC3b-opsonized particles was CR3-dependent. Adherent, interleukin-8 treated primary human neutrophils were treated with blocking antibodies against CD11b (ICRF44, 44a) or CD18 (TS1/18), or matched isotype controls, then exposed to inert carboxylate beads that were opsonized with iC3b. After 1 hour, cells were fixed and processed for imaging flow cytometry, using an analysis protocol that combines a spot count algorithm and step gate to quantify the binding and internalization of cargo across thousands of cells [43]. Coupling of iC3b to the beads was confirmed by imaging flow cytometry (Fig. 1A). As expected, association with and internalization of iC3b-opsonized beads by neutrophils was significantly inhibited by CR3 blockade (Fig. 1B–C). Functionality of the CR3 antibodies was confirmed by their ability to inhibit phagocytosis of complement-opsonized sheep erythrocytes (Fig. S1A–C), and CD11b remained on the neutrophil surface after treatment with anti-CD11b antibodies (Fig. S1D).

The fate of iC3b-opsonized beads and their ability to activate neutrophils were evaluated in comparison to the fate of beads that were opsonized with iC3b, followed by IgG that specifically recognizes human iC3b (Fig. 1A) [45]. iC3b+IgG beads served as a positive control for cargo that stimulates neutrophil ROS production and primary granule release via Fc γ receptors [31]. Phagosomes containing iC3b-opsonized beads were significantly less enriched for the primary granule protein neutrophil elastase than beads opsonized with iC3b+IgG (Fig. 1D–E). There was no difference in enrichment of the secondary granule protein lactoferrin on phagosomes between the two bead conditions (Fig. 1D–E). iC3b-opsonized beads induced a minimal ROS response in primary human neutrophils that was identical to what was observed for unopsonized beads, which was less than the response to beads opsonized with iC3b+IgG (Fig. 1F). These findings demonstrate that phagocytosis via CR3 alone weakly activates neutrophil antimicrobial activities.

CR3 mediates neutrophil phagocytosis of unopsonized Opa-negative *N. gonorrhoeae*.

We previously reported that unopsonized, Opa-negative Ngo does not elicit neutrophil ROS and is phagocytosed by adherent neutrophils into primary granule-negative phagosomes, in which they survive [31–33, 47]. We tested the hypothesis that Opa-negative Ngo uses CR3 as a phagocytic receptor based on three findings: 1) Complement (serum)-opsonized Ngo also does not elicit ROS from human neutrophils; 2) The percentage of Opa-negative Ngo in immature, elastase-negative phagosomes in adherent human neutrophils is similar

to what we observed for serum-opsonized Ngo and for iC3b-opsonized beads (Fig. 1) [48]; 3) CR3 has been reported as a phagocytic receptor for Ngo in primary cervical epithelial cells [9, 49, 50]. To test this hypothesis, adherent, interleukin-8 treated primary human neutrophils were treated with blocking antibodies against CD11b or CD18, or matched isotype controls, and then exposed to piliated Ngo of strain FA1090 in which all *opa* genes were deleted (Δ *opa*) [33]. Δ *opa* Ngo was used to limit the potential for variability in results due to Opa phase variation. Approximately 8–20% of adherent neutrophils had associated or internalized unopsonized Δ *opa* Ngo in the absence of blocking antibody, which is consistent with previous reports from our group [31–33, 51] and reflects the reduced efficiency of uptake of Ngo that are not opsonized or do not express Opa proteins (reviewed in [19, 52]).

Treatment with an antibody against the CD18 β subunit of CR3 significantly reduced both the percent of adherent human neutrophils with intracellular, unopsonized Δ *opa* Ngo (Fig. 2A) and the percent of neutrophils with associated (bound and internalized) bacteria (Fig. 2B). Similarly, treatment with an antibody against CD11b (44a [53]) significantly inhibited bacterial association and internalization by adherent human neutrophils (Fig. 2A–B). This result was not specific to Δ *opa* Ngo, as CR3 blocking antibodies also reduced association of neutrophils with predominantly Opa-negative Ngo of the FA1090 RM11.2, MS11 VD300, and 1291 strain backgrounds (Fig. S2A). The extent of association and phagocytosis of unopsonized Δ *opa* Ngo was low (~5–15% of neutrophils having Neutrophil association with and internalization of Δ *opa* Ngo was unaffected by blocking antibodies against CD11a and CD11c (Fig. 2C, Fig. S2B), which dimerize with CD18 and are also expressed on the neutrophil surface (Fig. S1E). Antibody-mediated blockade of human CEACAMs, which are present on the neutrophil surface (Fig. S1F) and bind Opa proteins [52], also had no effect on the association and internalization of Δ *opa* Ngo by neutrophils. However, anti-CEACAM antibody inhibited neutrophil association with and phagocytosis of FA1090 Ngo that constitutively expresses the CEACAM1- and CEACAM3-binding OpaD protein (OpaD+) in a statistically significant manner (Fig. 2D, Fig. S2C). CR3-blocking antibodies did not significantly affect the interaction of OpaD+ bacteria with neutrophils, suggesting Opa-CEACAM engagement is dominant over the interaction of Ngo with CR3 (Fig. 2D, Fig. S2C).

Although Ngo is a human-specific pathogen, CR3 is conserved among vertebrates (87.0% similarity and 74.8% identity between *Homo sapiens* (P11215) and *Mus musculus* (E9Q6O4) CD11b). We found that adherent murine neutrophils isolated from bone marrow also bound and phagocytosed Δ *opa* Ngo (Fig. 2E–F, Fig. S3A–B). The association and internalization of Δ *opa* Ngo with mouse neutrophils was significantly reduced upon treatment with anti-CD11b M170 antibody (Fig. 2E, Fig. S3C). Similarly, mouse neutrophils that are genetically deficient for CD11b interacted significantly less with Δ *opa* Ngo than wild-type neutrophils (Fig. 2F, Fig. S3D). Thus CD11b facilitates phagocytosis of adherent Ngo by both human and mouse neutrophils.

The 44a antibody targets a region of human CD11b comprising the I-domain and contributing to the metal ion-dependent adhesion site (MIDAS) motif that is formed upon release of CR3 from an inactive conformation [6, 53]. Treatment with the ICRF4 antibody, also directed against the I-domain of active CD11b, significantly reduced Ngo association

and internalization by adherent human neutrophils; the M170 antibody, which also blocks the I-domain, particularly the region of CD11b that recognizes complement fragment iC3b, also reduced Ngo-neutrophil interactions, though not in a statistically significant manner (Fig. S4D–E). Treatment of adherent human neutrophils with neutrophil inhibitory factor (NIF), a canine hookworm protein that binds the CD11b I-domain [54, 55], significantly reduced the association and internalization of opa Ngo by human neutrophils (Fig. 3A, Fig. S2F). In HL-60 human promyelocytes, which have low levels of surface CD11b, overexpression of full-length CD11b, but not CD11b lacking the I-domain, enhanced phagocytosis of opa Ngo, though not in a statistically significant manner (Fig. 3B). These results indicate that binding and phagocytosis of Ngo by human neutrophils use the MIDAS and I-domain of CD11b.

Neutrophils can make and release complement factors [56–62]. However, we did not detect deposition of C3 or C3-derived products on opa Ngo that was incubated with primary human or mouse neutrophils (Fig. 4A, C). Ngo incubated with the degranulated supernatant from human and mouse neutrophils also did not show surface C3 reactivity, including when degranulation was stimulated with the peptide fMLF (Fig. 4B–D). We verified the ability to detect complement C3 fragments on opa Ngo by opsonizing the bacteria in normal human or mouse serum (Fig. 4B–D). Serum opsonization enhanced bacterial phagocytosis by neutrophils, which was significantly reduced by addition of anti-CD11b antibody (Fig. 4E). On cervical cells, Ngo interacts directly with CR3 not only via C3 deposition, but also independently of complement through porin and the glycans on type IV pili [9, 63]. CD11b blockade significantly reduced the binding and phagocytosis of the piliated parental opa Ngo and an isogenic, hyperpiliated mutant (*pilT*) (Fig. S4A–B). Nonpiliated Ngo (inactivating mutations in the major pilin subunit *pilE* or the pilus secretin *pilQ*) was poorly internalized by neutrophils when compared with the piliated parent, such that any further reduction in internalization by the anti-CD11b antibody was unable to be accurately measured (Fig. S4A–B). Increasing the multiplicity of infection of *pilE* Ngo enhanced bacterial phagocytosis by neutrophils and was significantly inhibited when CD11b was blocked (Fig. S4C). CD11b blocking also significantly reduced the association and internalization of piliated, opa Ngo that does not glycosylate pilin, due to mutations in *pglA* or *pglD* (Fig. S4D–E). Thus pili enhance the interaction between Ngo and adherent neutrophils, but phagocytosis of non-piliated Ngo is still inhibited by blocking CR3.

Taken together, these results indicate that phagocytosis of Opa-negative Ngo by adherent neutrophils and neutrophil-like cells uses the CR3 integrin heterodimer, mediated by a region overlapping with the I-domain and MIDAS of CD11b, in a complement-independent manner.

Activation of CR3 is sufficient to mediate phagocytosis of Opa-negative *N. gonorrhoeae*.

Adherent, IL-8 treated neutrophils phagocytose Opa-negative Ngo, albeit less effectively than they phagocytose Opa+ bacteria [30, 31, 33, 48]. In contrast, many previous studies reported that neutrophils cannot phagocytose Opa-negative Ngo [21, 23, 28, 64]. Notably, these previous studies used neutrophils in suspension and without chemokine treatment, which would keep the cells in a quiescent, inactive state. Thus we hypothesized that Opa-

negative Ngo is not phagocytosed by neutrophils in suspension because they have less active surface CR3 than adherent cells. Supporting this hypothesis, primary human neutrophils in suspension had significantly less CD11b on their surface, as well as less CD11b in its active, ligand-binding conformation, compared to adherent, IL-8 treated neutrophils (Fig. 5A). Treatment of suspension neutrophils with phorbol myristate acetate (PMA) significantly increased the amount of surface CD11b in an active conformation, without affecting total surface CD11b (Fig. 5B). PMA treatment of suspension neutrophils significantly increased their association with (Fig. S5A) and internalization of opa Ngo (Fig. 5C–D). Addition of CD11b blocking antibody ablated this increase (Fig. 5C–D, Fig. S5A). In contrast, OpaD+ Ngo was bound and internalized by neutrophils in suspension and was unaffected by CD11b blockade (Fig. S5B–D), in keeping with numerous reports that suspension neutrophils phagocytose unopsonized Opa+ Ngo [20, 21, 23, 28, 29, 64–66]. These results indicate that phagocytosis of unopsonized, Opa-negative Ngo requires surface-presented CD11b in its active conformation, which is found in adherent and chemokine-primed neutrophils, but not in untreated neutrophils in suspension.

CR3 activation and stabilization of its active high affinity conformation requires the binding of its β integrin tail to talin, which connects the receptor to vinculin and the actin cytoskeleton [6]. At 10 min post infection, most opa bacteria were surface-bound and colocalized with endogenous talin in adherent, IL-8 treated human neutrophils (Fig. 5E). Colocalization was lost at 60 min post-infection, when opa Ngo had been phagocytosed (Fig. 5E). Based on all of these findings, we conclude that adherent, chemokine-treated neutrophils present CR3 in an active conformation that is necessary to mediate binding and phagocytosis of Opa-negative Ngo.

CR3-dependent phagocytosis is a “silent entry” mechanism of neutrophils.

We and others previously reported that Opa-negative Ngo does not stimulate neutrophil ROS production and is found in phagosomes that exhibit delayed fusion with primary granules to enable its intracellular survival [28, 31, 48, 51, 67]. To extend these observations, we monitored granule exocytosis and signaling events in adherent, IL-8 treated human neutrophils following exposure to Ngo. There was significantly less surface expression of CD63 on neutrophils that were exposed to opa compared with OpaD+ Ngo, indicating a reduction in primary granule exocytosis (Fig. 6A,C). Secondary granule exocytosis, as revealed by CD66b surface exposure, was not significantly different between opa and OpaD+ Ngo (Fig. 6B,C). This agrees with our report that Opa- and Opa+ Ngo phagosomes fuse similarly with secondary granules [31]. Neutrophils exposed to opa Ngo exhibited less phosphorylation of the intracellular signaling kinases Akt, p38, and Erk1/2, compared to those exposed to OpaD+ bacteria at matched time points (Fig. 6D–I). Together, these results connect CR3-mediated phagocytosis of Ngo to a reduced activation state of neutrophils.

To extend these results to an unrelated bacterium, we turned to *Mycobacterium smegmatis*, which is reported to be internalized by neutrophils via CR3 and does not induce primary granule exocytosis [68]. We adapted the imaging flow cytometry protocol described above to quantify *M. smegmatis* internalization using a pixel erode mask from the cell boundary (Fig. S6). Phagocytosis of non-opsonized *M. smegmatis* by adherent, IL-8 treated human

neutrophils was significantly inhibited when CD18 was blocked (Fig. 7A). Enrichment of neutrophil elastase around *M. smegmatis* phagosomes after 1 hr infection was lower than for opa Ngo, and both *M. smegmatis* and opa phagosomes were significantly less elastase positive than phagosomes containing OpaD+ Ngo (Fig. 7B–C). Like opa Ngo, *M. smegmatis* did not stimulate neutrophil ROS production, in contrast to the strong ROS response elicited by OpaD+ Ngo (Fig. 7D) [33, 47].

Together, the results with Ngo, iC3b-opsonized beads, and *M. smegmatis* support a model in which CR3 engagement facilitates phagocytosis of diverse cargo with incomplete neutrophil activation, and this is exploited by pathogens to evade full neutrophil antimicrobial activity (Fig. 8).

DISCUSSION

CR3 is a prominent phagocytic receptor on vertebrate phagocytes, including neutrophils. Despite extensive research on how CR3 is activated to mediate phagocytosis, the downstream consequences of CR3-mediated phagocytosis remain uncertain. Here, we use iC3b-opsonized polystyrene beads to show that phagocytosis solely by CR3 in neutrophils does not elicit a prominent ROS response or primary granule release. The same phenotypes are found for neutrophil CR3-binding *M. smegmatis*. For the first time, we identify CR3 as the main phagocytic receptor on neutrophils for Ngo that is not opsonized or lacks other adhesins (e.g. phase variable Opa proteins). Phagocytosis of Ngo requires the I-domain and MIDAS of CD11b, and placement of CR3 into an active conformation that is only achieved in adherent, primed neutrophils, and not for unstimulated neutrophils in suspension. CR3-mediated phagocytosis of Opa-negative Ngo was linked to a less activated state of neutrophils, with reduced activation of protein kinases implicated in proinflammatory signaling, less granule fusion with the cell surface (less degranulation) and phagosomes (less phagosome maturation), and minimal ROS production. These results with three unrelated phagocytic cargo define CR3-mediated phagocytosis as a pathway of “silent entry” into neutrophils, which is exploited by pathogens like Ngo and Msm to create an intracellular niche that supports their survival (Fig. 8).

Despite decades of study on CR3, there are conflicting results regarding the downstream fate of cargo that engage CR3 on phagocytes. iC3b-opsonized zymosan, a common experimental substrate for neutrophils, induces a potent ROS and degranulation response [69]. However, zymosan is also recognized by dectin receptors that activate neutrophils [70, 71]. The β -glucan of zymosan also interacts directly with the lectin domain of CD11b [69]. Erythrocytes coated with either C3b or iC3b are phagocytosed but do not induce ROS generation in human monocytes and neutrophils [72]. In contrast, C3 and iC3b-coated latex beads are reported to elicit neutrophil ROS [73]. Here, we found that iC3b-opsonized polystyrene beads, in the absence of any other ligands, are phagocytosed by neutrophils into immature phagosomes and do not induce ROS production. Given the results with zymosan, we suggest that inconsistencies in the literature regarding CR3-mediated phagocytosis and neutrophil activation are attributable to other surface features of the phagocytosed target, or the presence of other soluble components that opsonize the target or stimulate neutrophils. For instance, binding of C5a, the cleavage product of complement component

5, to the C5a receptor on neutrophils leads to upregulation of CR3 on neutrophils, and consequent ROS production [74–76]. It is intriguing that pathogen-associated molecular patterns on opa Ngo do not activate neutrophils in the infection condition used here, although Ngo lipooligosaccharide is a ligand for TLR4 and its PorB porin binds TLR2 [77, 78]. In macrophages, engagement of CR3 by complement-opsonized *Francisella tularensis* downregulates TLR2 responses to dampen proinflammatory signaling [79]. If this is a general approach used by microbes that target CR3, then bacteria as unrelated as Ngo and Msm would be expected to exploit CR3 not just to access an intracellular niche in phagocytes that lacks full degradative capacity, but also to lessen the host-protective inflammatory response.

How Ngo interacts with CR3 on neutrophils is not currently known. We did not detect any deposition of C3 on Ngo that was incubated with neutrophils or degranulated neutrophil supernatant (Fig. 4). This is in contrast to the action of primary human cervical cells, which release C3 that covalently reacts with Ngo lipooligosaccharide [80]. Ngo also did not use its pili to mediate CR3 binding and phagocytosis by adherent neutrophils (Fig. S4). Here, pili may be dispensable because CR3 is already in its active conformation on adherent, IL-8 treated neutrophils, whereas in cervical cells, the interaction of glycosylated pili with CR3 is required to activate CR3 [63]. The interaction between cervical CR3 and Ngo involves a cooperative synergy with pili and porin [50]. However, we were unable to test a role for porin in CR3-mediated phagocytosis by neutrophils because porin is essential in Ngo. The monoclonal antibody that recognizes FA1090 porin cannot be processed into F'(ab) fragments for blocking, and the intact antibody would opsonize the bacteria for phagocytosis via Fc receptors. We envision three possibilities to explain how opa Ngo uses CR3 on neutrophils for phagocytosis. First, Ngo surface structures other than pili and porin directly engage CR3. For instance, in the related pathogen *Neisseria meningitidis*, lipooligosaccharide interacts with CR3 [81]. Second, Ngo binds a neutrophil-derived protein such as LL-37 or myeloperoxidase, which have been reported as ligands for CR3 [13, 82]. Third, CR3 signaling may be required for activation of another receptor that drives Ngo phagocytosis by neutrophils, or for stimulating actin-dependent membrane ruffling and bacterial uptake by macropinocytosis. In all cases, the consequence would be phagocytosis without ROS production or full degranulation, and ineffective bacterial killing.

While neutrophils in suspension cannot phagocytose unopsonized, Opa-negative Ngo, neutrophils that are adherent and treated with IL-8 can [28–31, 33, 64, 83]. These discordant results can be explained by our finding that neutrophils in suspension have reduced levels of CR3 on their surface, including CR3 in its active ligand-binding conformation, compared to adherent and primed neutrophils. In circulation, CR3 is inactive to prevent indiscriminate binding of phagocytes to endothelial cells. Both inside-out and outside-in signals, including attachment to extracellular matrix proteins such as fibronectin, activate CR3 on phagocytes [5, 6]. We found that treating neutrophils in suspension with PMA, a PKC activator known to promote CR3 activation [84], was sufficient to increase phagocytosis of opa Ngo in a CR3-dependent manner (Fig. 5). This result highlights the importance of the physiological state of immune cells in host-pathogen interactions. Notably, adherent neutrophils required PMA treatment in order to phagocytose iC3b-coated beads or erythrocytes, but they successfully phagocytosed Ngo and *M. smegmatis*. This result may indicate that a second

signal, such as a microbe-associated molecular pattern on the bacterial surface, is required for inside-out signaling to place neutrophil CR3 in an active phagocytosis-competent state. Alternatively, Ngo and *M. smegmatis* may interact with a slightly different domain of CR3 than iC3b. This possibility is supported by the differential effects of the anti-CD11b blocking antibodies 44a and M170 on neutrophil phagocytosis of opa Ngo, compared with iC3b-opsonized sRBCs (Fig. 2, Fig. S2D–E). M170 had a more prominent effect on phagocytosis by mouse neutrophils compared with human neutrophils, which could be due to a higher affinity of this antibody for mouse vs. human CD11b, or differences in the activation state of CR3 in mouse vs. human neutrophils in our experimental conditions. Anti-CEACAM antibody reduced phagocytosis of OpaD+ Ngo by neutrophils to what was measured for opa Ngo without CR3 blocking (Fig. 2D). This result implies that CR3 and CEACAM independently drive neutrophil phagocytosis of Opa-negative or Opa+ Ngo, respectively. This scenario differs from IgG receptor signaling, where CR3 synergizes with Fc γ receptors to promote rapid phagocytosis and degradation of substrates [85]. The dynamics between CR3 and other phagocytic receptors, particularly CEACAMs, in neutrophil phagocytosis, and how additional cargo-derived signals affect phagocytosis, warrants further investigation. However, these questions will require a more genetically tractable system than primary human neutrophils, which are terminally differentiated.

Diverse pathogens, as well as their secreted toxins and virulence factors, interact with CR3 in a complement-independent manner [7, 8, 14, 68, 79, 81, 86–91]. This study directly connects engagement of CR3 to evasion of phagocyte activation and phagocytic clearance, which we are terming “silent entry.” Furthermore, it identifies CR3 as a participant in a pathway that is exploited by *M. smegmatis* and Ngo to be taken up by and survive inside neutrophils. This may help explain the clinical observation that neutrophils in human gonorrheal exudates contain intact intracellular Ngo [19]. Our work is in agreement with reports that the phagocytosis of *Mycobacterium smegmatis*, *M. kansasii*, and *M. tuberculosis* by neutrophils or macrophages uses CR3 and does not lead to ROS production or phagosome maturation [14, 68, 86, 92–96]. Similarly, *Leishmania* prevents ROS production and phagolysosome formation in phagocytes in a CR3-dependent manner to enable its survival [97, 98], and macrophages infected with complement-opsonized *F. tularensis* have limited pro-inflammatory signaling and cytokine production [79, 99]. However, our work with OpaD+ Ngo suggests that the exploitation of CR3 by pathogens can be overcome by ectopically activating ITAM-bearing receptors such as Fc γ receptors, dectins, and CEACAM3, which send signals that activate phagocytes alongside or independently of CR3 [6, 85, 100, 101]. Vaccination or host-directed therapies can therefore be used to target the phagocytes that are recruited to sites of infection in order to thwart this silent entry pathway and therefore enhance pathogen clearance.

Supplementary Material

Refer to Web version on PubMed Central for supplementary material.

ACKNOWLEDGEMENTS

We thank Michael Solga and Joanne Lannigan (University of Virginia Flow Cytometry Core, RRID: SCR_017829) for their advice on imaging flow cytometry. We thank Michael Apicella, Jennifer Edwards, Girija Ramakrishnan,

Hank Seifert, and Christina Stallings for strains and mutant constructs, Victor Torres for HL-60 cell lines, and Larry Schlesinger for helpful discussions. We thank CJ Anderson, Borna Mehrad, and Kathy Michaels for advice on isolation and immunofluorescence of mouse neutrophils, and Jeff Teoh for assistance with establishing flow cytometry protocols. We thank Marieke Jones for advice on statistical analyses and Allison Alcott for assistance with manual quantitation. This work was supported by NIH R01 AI097312, the University of Virginia School of Medicine Pinn Scholar Award, and the Department of Microbiology, Immunology, and Cancer Biology to AKC. SAR was supported in part by NIH T32 AI007046. SAR and LMW were supported in part by the Robert R. Wagner Fellowship, University of Virginia. KPD was supported in part by the University of Virginia's Harrison Undergraduate Research Fellowship and Hutcheson Family Fellowship. Human subjects gave informed consent and participated in research according to a protocol approved by the University of Virginia Institutional Review Board for Health Sciences Research. Research with animals was conducted according to a protocol approved by the University of Virginia Animal Care and Use Committee.

ABBREVIATIONS

ANOVA	analysis of variance
CEACAM	carcinoembryonic antigen-related cell adhesion molecule
CFSE	carboxyfluorescein diacetate succinimidyl ester
CR3	complement receptor 3
IL-8	interleukin-8
ITAM	immunotyrosine-based activation motif
MIDAS	metal ion-dependent adhesion site
MOI	multiplicity of infection
Ngo	<i>Neisseria gonorrhoeae</i>
NIF	neutrophil inhibitory factor
Opa	opacity-associated protein
PBS	phosphate-buffered saline
PFA	paraformaldehyde
PMA	phorbol myristate acetate
ROS	reactive oxygen species

REFERENCES

1. Uribe-Querol E and Rosales C (2020) Phagocytosis: Our Current Understanding of a Universal Biological Process. *Front Immunol* 11, 1066. [PubMed: 32582172]
2. Yin C and Heit B (2018) Armed for destruction: formation, function and trafficking of neutrophil granules. *Cell Tissue Res* 371, 455–71. [PubMed: 29185068]
3. Nauseef WM (2019) The phagocyte NOX2 NADPH oxidase in microbial killing and cell signaling. *Curr Opin Immunol* 60, 130–40. [PubMed: 31302569]
4. Burn GL, Foti A, Marsman G, Patel DF, Zychlinsky A (2021) The Neutrophil. *Immunity* 54, 1377–91. [PubMed: 34260886]

5. Lamers C, Pluss CJ, Ricklin D (2021) The Promiscuous Profile of Complement Receptor 3 in Ligand Binding, Immune Modulation, and Pathophysiology. *Front Immunol* 12, 662164. [PubMed: 33995387]
6. Lim J and Hotchin NA (2012) Signalling mechanisms of the leukocyte integrin alphaMbeta2: current and future perspectives. *Biol Cell* 104, 631–40. [PubMed: 22804617]
7. Eby JC, Gray MC, Mangan AR, Donato GM, Hewlett EL (2012) Role of CD11b/CD18 in the process of intoxication by the adenylate cyclase toxin of *Bordetella pertussis*. *Infect Immun* 80, 850–9. [PubMed: 22144488]
8. DuMont AL, Yoong P, Day CJ, Alonzo F 3rd, McDonald WH, Jennings MP, Torres VJ (2013) *Staphylococcus aureus* LukAB cytotoxin kills human neutrophils by targeting the CD11b subunit of the integrin Mac-1. *Proc Natl Acad Sci USA* 110, 10794–9. [PubMed: 23754403]
9. Edwards JL and Apicella MA (2005) I-domain-containing integrins serve as pilus receptors for *Neisseria gonorrhoeae* adherence to human epithelial cells. *Cell Microbiol* 7, 1197–211. [PubMed: 16008586]
10. van Bruggen R, Zweers D, van Diepen A, van Dissel JT, Roos D, Verhoeven AJ, Kuijpers TW (2007) Complement receptor 3 and Toll-like receptor 4 act sequentially in uptake and intracellular killing of unopsonized *Salmonella enterica* serovar Typhimurium by human neutrophils. *Infect Immun* 75, 2655–60. [PubMed: 17353285]
11. Wright SD, Levin SM, Jong MT, Chad Z, Kabbash LG (1989) CR3 (CD11b/CD18) expresses one binding site for Arg-Gly-Asp-containing peptides and a second site for bacterial lipopolysaccharide. *J Exp Med* 169, 175–83. [PubMed: 2462607]
12. Ross GD (2000) Regulation of the adhesion versus cytotoxic functions of the Mac-1/CR3/alphaMbeta2-integrin glycoprotein. *Crit Rev Immunol* 20, 197–222. [PubMed: 10968371]
13. Lishko VK, Moreno B, Podolnikova NP, Ugarova TP (2016) Identification of Human Cathelicidin Peptide LL-37 as a Ligand for Macrophage Integrin alphaMbeta2 (Mac-1, CD11b/CD18) that Promotes Phagocytosis by Opsonizing Bacteria. *Res Rep Biochem* 2016, 39–55. [PubMed: 27990411]
14. Peyron P, Bordier C, N'Diaye EN, Maridonneau-Parini I (2000) Nonopsonic phagocytosis of *Mycobacterium kansasii* by human neutrophils depends on cholesterol and is mediated by CR3 associated with glycosylphosphatidylinositol-anchored proteins. *J Immunol* 165, 5186–91. [PubMed: 11046051]
15. Orrskog S, Rounioja S, Spadafina T, Gallotta M, Norman M, Hentrich K, Falker S, Ygberg-Eriksson S, Hasenberg M, Johansson B, Uotila LM, Gahmberg CG, Barocchi M, Gunzer M, Normark S, Henriques-Normark B (2012) Pilus adhesin RrgA interacts with complement receptor 3, thereby affecting macrophage function and systemic pneumococcal disease. *mBio* 4, e00535–12. [PubMed: 23269830]
16. Mayadas TN and Cullere X (2005) Neutrophil beta2 integrins: moderators of life or death decisions. *Trends Immunol* 26, 388–95. [PubMed: 15922663]
17. Allen LH and Criss AK (2019) Cell intrinsic functions of neutrophils and their manipulation by pathogens. *Curr Opin Immunol* 60, 124–29. [PubMed: 31302568]
18. Quillin SJ and Seifert HS (2018) *Neisseria gonorrhoeae* host adaptation and pathogenesis. *Nat Rev Microbiol* 16, 226–40. [PubMed: 29430011]
19. Palmer A and Criss AK (2018) Gonococcal Defenses against Antimicrobial Activities of Neutrophils. *Trends Microbiol* 26, 1022–34. [PubMed: 30115561]
20. Swanson J, Sparks E, Zeligs B, Siam MA, Parrott C (1974) Studies on gonococcus infection. V. Observations on in vitro interactions of gonococci and human neutrophils. *Infect Immun* 10, 633–44. [PubMed: 4214776]
21. Gray-Owen SD, Dehio C, Haude A, Grunert F, Meyer TF (1997) CD66 carcinoembryonic antigens mediate interactions between Opa-expressing *Neisseria gonorrhoeae* and human polymorphonuclear phagocytes. *EMBO J* 16, 3435–45. [PubMed: 9218786]
22. Chen T, Grunert F, Medina-Marino A, Gotschlich EC (1997) Several carcinoembryonic antigens (CD66) serve as receptors for gonococcal opacity proteins. *J Exp Med* 185, 1557–64. [PubMed: 9151893]

23. Virji M, Makepeace K, Ferguson DJ, Watt SM (1996) Carcinoembryonic antigens (CD66) on epithelial cells and neutrophils are receptors for Opa proteins of pathogenic neisseriae. *Mol Microbiol* 22, 941–50. [PubMed: 8971715]
24. Kuespert K, Pils S, Hauck CR (2006) CEACAMs: their role in physiology and pathophysiology. *Curr Opin Cell Biol* 18, 565–71. [PubMed: 16919437]
25. Schmitter T, Agerer F, Peterson L, Munzner P, Hauck CR (2004) Granulocyte CEACAM3 is a phagocytic receptor of the innate immune system that mediates recognition and elimination of human-specific pathogens. *J Exp Med* 199, 35–46. [PubMed: 14707113]
26. McCaw SE, Schneider J, Liao EH, Zimmermann W, Gray-Owen SD (2003) Immunoreceptor tyrosine-based activation motif phosphorylation during engulfment of *Neisseria gonorrhoeae* by the neutrophil-restricted CEACAM3 (CD66d) receptor. *Mol Microbiol* 49, 623–37. [PubMed: 12864848]
27. Alcott AM, Werner LM, Baiocco CM, Belcher Dufresne M, Columbus L, Criss AK (2022) Variable Expression of Opa Proteins by *Neisseria gonorrhoeae* Influences Bacterial Association and Phagocytic Killing by Human Neutrophils. *J Bacteriol* 204, e0003522. [PubMed: 35343795]
28. Fischer SH and Rest RF (1988) Gonococci possessing only certain P.II outer membrane proteins interact with human neutrophils. *Infection and immunity* 56, 1574–9. [PubMed: 3131247]
29. Virji M and Heckels JE (1986) The effect of protein II and pili on the interaction of *Neisseria gonorrhoeae* with human polymorphonuclear leucocytes. *J Gen Microbiol* 132, 503–12. [PubMed: 2872268]
30. Criss AK, Katz BZ, Seifert HS (2009) Resistance of *Neisseria gonorrhoeae* to non-oxidative killing by adherent human polymorphonuclear leucocytes. *Cell Microbiol* 11, 1074–87. [PubMed: 19290914]
31. Johnson MB and Criss AK (2013) *Neisseria gonorrhoeae* phagosomes delay fusion with primary granules to enhance bacterial survival inside human neutrophils. *Cell Microbiol* 15, 1323–40. [PubMed: 23374609]
32. Smirnov A, Daily KP, Criss AK (2013) Assembly of NADPH Oxidase in Human Neutrophils Is Modulated by the Opacity-Associated Protein Expression State of *Neisseria gonorrhoeae*. *Infect Immun* 82, 1036–44. [PubMed: 24343654]
33. Ball LM and Criss AK (2013) Constitutively Opa-expressing and Opa-deficient *Neisseria gonorrhoeae* strains differentially stimulate and survive exposure to human neutrophils. *J Bacteriol* 195, 2982–90. [PubMed: 23625842]
34. Long CD, Madraswala RN, Seifert HS (1998) Comparisons between colony phase variation of *Neisseria gonorrhoeae* FA1090 and pilus, pilin, and S-pilin expression. *Infect Immun* 66, 1918–27. [PubMed: 9573070]
35. Ragland SA, Schaub RE, Hackett KT, Dillard JP, Criss AK (2017) Two lytic transglycosylases in *Neisseria gonorrhoeae* impart resistance to killing by lysozyme and human neutrophils. *Cell Microbiol* 19.
36. Achtman M, Neibert M, Crowe BA, Strittmatter W, Kusecek B, Weyse E, Walsh MJ, Slawig B, Morelli G, Moll A, et al. (1988) Purification and characterization of eight class 5 outer membrane protein variants from a clone of *Neisseria meningitidis* serogroup A. *J Exp Med* 168, 507–25. [PubMed: 2457646]
37. Kellogg DS Jr., Peacock WL Jr., Deacon WE, Brown L, Pirkle DI (1963) *Neisseria Gonorrhoeae*. I. Virulence Genetically Linked to Clonal Variation. *J Bacteriol* 85, 1274–9. [PubMed: 14047217]
38. Ragland SA and Criss AK (2019) Protocols to Interrogate the Interactions Between *Neisseria gonorrhoeae* and Primary Human Neutrophils. *Methods Mol Biol* 1997, 319–45. [PubMed: 31119632]
39. Carroll P, Schreuder LJ, Muwanguzi-Karugaba J, Wiles S, Robertson BD, Ripoll J, Ward TH, Bancroft GJ, Schaible UE, Parish T (2010) Sensitive detection of gene expression in mycobacteria under replicating and non-replicating conditions using optimized far-red reporters. *PLoS One* 5, e9823. [PubMed: 20352111]
40. Tan S, Sukumar N, Abramovitch RB, Parish T, Russell DG (2013) *Mycobacterium tuberculosis* responds to chloride and pH as synergistic cues to the immune status of its host cell. *PLoS Pathog* 9, e1003282. [PubMed: 23592993]

41. Dillard JP (2006) Genetic manipulation of *Neisseria gonorrhoeae*. *Curr Protoc Microbiol* Chapter 4, Unit 4A 2.
42. Long CD, Tobiasson DM, Lazio MP, Kline KA, Seifert HS (2003) Low-level pilin expression allows for substantial DNA transformation competence in *Neisseria gonorrhoeae*. *Infect Immun* 71, 6279–91. [PubMed: 14573647]
43. Smirnov A, Solga MD, Lannigan J, Criss AK (2020) Using Imaging Flow Cytometry to Quantify Neutrophil Phagocytosis. *Methods Mol Biol* 2087, 127–40. [PubMed: 31728988]
44. Chow CW, Downey GP, Grinstein S (2004) Measurements of phagocytosis and phagosomal maturation. *Curr Protoc Cell Biol* Chapter 15, Unit 15 7.
45. DiLillo DJ, Pawluczko AW, Peng W, Kennedy AD, Beum PV, Lindorfer MA, Taylor RP (2006) Selective and efficient inhibition of the alternative pathway of complement by a mAb that recognizes C3b/iC3b. *Mol Immunol* 43, 1010–9. [PubMed: 15961157]
46. Werner LM, Palmer A, Smirnov A, Belcher Dufresne M, Columbus L, Criss AK (2020) Imaging Flow Cytometry Analysis of CEACAM Binding to Opa-Expressing *Neisseria gonorrhoeae*. *Cytometry A* 97, 1081–9. [PubMed: 32484607]
47. Criss AK and Seifert HS (2008) *Neisseria gonorrhoeae* suppresses the oxidative burst of human polymorphonuclear leukocytes. *Cell Microbiol* 10, 2257–70. [PubMed: 18684112]
48. Johnson MB, Ball LM, Daily KP, Martin JN, Columbus L, Criss AK (2015) Opa+ *Neisseria gonorrhoeae* exhibits reduced survival in human neutrophils via Src family kinase-mediated bacterial trafficking into mature phagolysosomes. *Cell Microbiol* 17, 648–65. [PubMed: 25346239]
49. Edwards JL, Brown EJ, Ault KA, Apicella MA (2001) The role of complement receptor 3 (CR3) in *Neisseria gonorrhoeae* infection of human cervical epithelia. *Cell Microbiol* 3, 611–22. [PubMed: 11553013]
50. Edwards JL, Brown EJ, Uk-Nham S, Cannon JG, Blake MS, Apicella MA (2002) A co-operative interaction between *Neisseria gonorrhoeae* and complement receptor 3 mediates infection of primary cervical epithelial cells. *Cell Microbiol* 4, 571–84. [PubMed: 12390350]
51. Smirnov A, Solga MD, Lannigan J, Criss AK (2015) An improved method for differentiating cell-bound from internalized particles by imaging flow cytometry. *J Immunol Methods* 423, 60–9. [PubMed: 25967947]
52. Sadarangani M, Pollard AJ, Gray-Owen SD (2011) Opa proteins and CEACAMs: pathways of immune engagement for pathogenic *Neisseria*. *FEMS Microbiol Rev* 35, 498–514. [PubMed: 21204865]
53. Arnaout MA, Todd RF 3rd, Dana N, Melamed J, Schlossman SF, Colten HR (1983) Inhibition of phagocytosis of complement C3- or immunoglobulin G-coated particles and of C3bi binding by monoclonal antibodies to a monocyte-granulocyte membrane glycoprotein (Mol). *J Clin Invest* 72, 171–9. [PubMed: 6874946]
54. Rieu P, Ueda T, Haruta I, Sharma CP, Arnaout MA (1994) The A-domain of beta 2 integrin CR3 (CD11b/CD18) is a receptor for the hookworm-derived neutrophil adhesion inhibitor NIF. *J Cell Biol* 127, 2081–91. [PubMed: 7528750]
55. Ustinov VA and Plow EF (2002) Delineation of the key amino acids involved in neutrophil inhibitory factor binding to the I-domain supports a mosaic model for the capacity of integrin alphaMbeta 2 to recognize multiple ligands. *J Biol Chem* 277, 18769–76. [PubMed: 11880366]
56. Botto M, Lissandrini D, Sorio C, Walport MJ (1992) Biosynthesis and secretion of complement component (C3) by activated human polymorphonuclear leukocytes. *J Immunol* 149, 1348–55. [PubMed: 1500721]
57. Faried HF, Tachibana T, Okuda T (1993) The secretion of the third component of complement (C3) by human polymorphonuclear leukocytes from both normal and systemic lupus erythematosus cases. *Scand J Immunol* 37, 19–28. [PubMed: 8418468]
58. Nguyen HX, Galvan MD, Anderson AJ (2008) Characterization of early and terminal complement proteins associated with polymorphonuclear leukocytes in vitro and in vivo after spinal cord injury. *J Neuroinflammation* 5, 26. [PubMed: 18578885]
59. Okuda T (1991) Murine polymorphonuclear leukocytes synthesize and secrete the third component and factor B of complement. *Int Immunol* 3, 293–6. [PubMed: 1878337]

60. Okuda T and Suzuki H (1996) Immunocytochemical Demonstration of C3 in Mouse Neutrophils and Eosinophils. *Acta Histochemica et Cytochemica* 29, 181–4.
61. Okuda T and Tachibana T (1992) Secretion and function of the third component of complement (C3) by murine leukocytes. *Int Immunol* 4, 681–90. [PubMed: 1616899]
62. Hogasen AK, Wurzner R, Abrahamsen TG, Dierich MP (1995) Human polymorphonuclear leukocytes store large amounts of terminal complement components C7 and C6, which may be released on stimulation. *J Immunol* 154, 4734–40. [PubMed: 7722325]
63. Jennings MP, Jen FE, Roddam LF, Apicella MA, Edwards JL (2011) Neisseria gonorrhoeae pili glycan contributes to CR3 activation during challenge of primary cervical epithelial cells. *Cell Microbiol* 13, 885–96. [PubMed: 21371235]
64. Rest RF, Fischer SH, Ingham ZZ, Jones JF (1982) Interactions of Neisseria gonorrhoeae with human neutrophils: effects of serum and gonococcal opacity on phagocyte killing and chemiluminescence. *Infect Immun* 36, 737–44. [PubMed: 6806195]
65. Chen T and Gotschlich EC (1996) CGM1a antigen of neutrophils, a receptor of gonococcal opacity proteins. *Proc Natl Acad Sci USA* 93, 14851–6. [PubMed: 8962144]
66. Kupsch EM, Knepper B, Kuroki T, Heuer I, Meyer TF (1993) Variable opacity (Opa) outer membrane proteins account for the cell tropisms displayed by Neisseria gonorrhoeae for human leukocytes and epithelial cells. *EMBO J* 12, 641–50. [PubMed: 8440254]
67. Nais FL and Rest RF (1991) Stimulation of human neutrophil oxidative metabolism by nonopsonized Neisseria gonorrhoeae. *Infect Immun* 59, 4383–90. [PubMed: 1657785]
68. Cougoule C, Constant P, Etienne G, Daffe M, Maridonneau-Parini I (2002) Lack of fusion of azurophil granules with phagosomes during phagocytosis of Mycobacterium smegmatis by human neutrophils is not actively controlled by the bacterium. *Infect Immun* 70, 1591–8. [PubMed: 11854248]
69. Ross GD, Cain JA, Lachmann PJ (1985) Membrane complement receptor type three (CR3) has lectin-like properties analogous to bovine conglutinin as functions as a receptor for zymosan and rabbit erythrocytes as well as a receptor for iC3b. *J Immunol* 134, 3307–15. [PubMed: 2984286]
70. Taylor PR, Tsoni SV, Willment JA, Dennehy KM, Rosas M, Findon H, Haynes K, Steele C, Botto M, Gordon S, Brown GD (2007) Dectin-1 is required for beta-glucan recognition and control of fungal infection. *Nat Immunol* 8, 31–8. [PubMed: 17159984]
71. Li X, Utomo A, Cullere X, Choi MM, Milner DA Jr., Venkatesh D, Yun SH, Mayadas TN (2011) The beta-glucan receptor Dectin-1 activates the integrin Mac-1 in neutrophils via Vav protein signaling to promote Candida albicans clearance. *Cell Host Microbe* 10, 603–15. [PubMed: 22177564]
72. Wright SD and Silverstein SC (1983) Receptors for C3b and C3bi promote phagocytosis but not the release of toxic oxygen from human phagocytes. *J Exp Med* 158, 2016–23. [PubMed: 6227677]
73. Hoogerwerf M, Weening RS, Hack CE, Roos D (1990) Complement fragments C3b and iC3b coupled to latex induce a respiratory burst in human neutrophils. *Mol Immunol* 27, 159–67. [PubMed: 2138709]
74. Lappégard KT, Christiansen D, Pharo A, Thorgersen EB, Hellerud BC, Lindstad J, Nielsen EW, Bergseth G, Fadnes D, Abrahamsen TG, Hoiby EA, Schejbel L, Garred P, Lambris JD, Harboe M, Mollnes TE (2009) Human genetic deficiencies reveal the roles of complement in the inflammatory network: lessons from nature. *Proc Natl Acad Sci USA* 106, 15861–6. [PubMed: 19717455]
75. Mollnes TE, Brekke OL, Fung M, Fure H, Christiansen D, Bergseth G, Videm V, Lappégard KT, Kohl J, Lambris JD (2002) Essential role of the C5a receptor in E coli-induced oxidative burst and phagocytosis revealed by a novel lepirudin-based human whole blood model of inflammation. *Blood* 100, 1869–77. [PubMed: 12176911]
76. Sprong T, Brandtzaeg P, Fung M, Pharo AM, Hoiby EA, Michaelsen TE, Aase A, van der Meer JW, van Deuren M, Mollnes TE (2003) Inhibition of C5a-induced inflammation with preserved C5b-9-mediated bactericidal activity in a human whole blood model of meningococcal sepsis. *Blood* 102, 3702–10. [PubMed: 12881318]

77. Massari P, Henneke P, Ho Y, Latz E, Golenbock DT, Wetzler LM (2002) Cutting edge: Immune stimulation by neisserial porins is toll-like receptor 2 and MyD88 dependent. *J Immunol* 168, 1533–7. [PubMed: 11823477]
78. Pridmore AC, Jarvis GA, John CM, Jack DL, Dower SK, Read RC (2003) Activation of toll-like receptor 2 (TLR2) and TLR4/MD2 by *Neisseria* is independent of capsule and lipooligosaccharide (LOS) sialylation but varies widely among LOS from different strains. *Infect Immun* 71, 3901–8. [PubMed: 12819075]
79. Dai S, Rajaram MV, Curry HM, Leander R, Schlesinger LS (2013) Fine tuning inflammation at the front door: macrophage complement receptor 3-mediates phagocytosis and immune suppression for *Francisella tularensis*. *PLoS Pathog* 9, e1003114. [PubMed: 23359218]
80. Edwards JL and Apicella MA (2002) The role of lipooligosaccharide in *Neisseria gonorrhoeae* pathogenesis of cervical epithelia: lipid A serves as a C3 acceptor molecule. *Cell Microbiol* 4, 585–98. [PubMed: 12390351]
81. Jones HE, Strid J, Osman M, Uronen-Hansson H, Dixon G, Klein N, Wong SY, Callard RE (2008) The role of beta2 integrins and lipopolysaccharide-binding protein in the phagocytosis of dead *Neisseria meningitidis*. *Cell Microbiol* 10, 1634–45. [PubMed: 18397383]
82. Johansson MW, Patarroyo M, Oberg F, Siegbahn A, Nilsson K (1997) Myeloperoxidase mediates cell adhesion via the alpha M beta 2 integrin (Mac-1, CD11b/CD18). *J Cell Sci* 110 (Pt 9), 1133–9. [PubMed: 9175709]
83. King GJ and Swanson J (1978) Studies on gonococcus infection. XV. Identification of surface proteins of *Neisseria gonorrhoeae* correlated with leukocyte association. *Infect Immun* 21, 575–84. [PubMed: 211086]
84. Wright SD, Craigmyle LS, Silverstein SC (1983) Fibronectin and serum amyloid P component stimulate C3b- and C3bi-mediated phagocytosis in cultured human monocytes. *J Exp Med* 158, 1338–43. [PubMed: 6225825]
85. Lindorfer MA, Kohl J, Taylor RP (2014) Interactions between the complement system and Fcγ receptors. In *Antibody Fc: Linking adaptive and innate immunity* (Ackerman ME and Nimmerjahn F, eds), Elsevier, London 49–74.
86. Schlesinger LS, Bellinger-Kawahara CG, Payne NR, Horwitz MA (1990) Phagocytosis of *Mycobacterium tuberculosis* is mediated by human monocyte complement receptors and complement component C3. *J Immunol* 144, 2771–80. [PubMed: 2108212]
87. Zimmerli S, Edwards S, Ernst JD (1996) Selective receptor blockade during phagocytosis does not alter the survival and growth of *Mycobacterium tuberculosis* in human macrophages. *Am J Resp Cell Mol Biol* 15, 760–70.
88. Uribe KB, Martín C, Etxebarria A, González-Bullón D, Gómez-Bilbao G, Ostolaza H (2013) Ca²⁺ influx and tyrosine kinases trigger *Bordetella adenylate cyclase toxin* (ACT) endocytosis. Cell physiology and expression of the CD11b/CD18 integrin major determinants of the entry route. *PLoS One* 8, e74248. [PubMed: 24058533]
89. Hawley KL, Olson CM Jr., Iglesias-Pedraz JM, Navasa N, Cervantes JL, Caimano MJ, Izadi H, Ingalls RR, Pal U, Salazar JC, Radolf JD, Anguita J (2012) CD14 cooperates with complement receptor 3 to mediate MyD88-independent phagocytosis of *Borrelia burgdorferi*. *Proc Natl Acad Sci USA* 109, 1228–32. [PubMed: 22232682]
90. Schlesinger LS and Horwitz MA (1990) Phagocytosis of leprosy bacilli is mediated by complement receptors CR1 and CR3 on human monocytes and complement component C3 in serum. *J Clin Invest* 85, 1304–14. [PubMed: 2138634]
91. Hajishengallis G, Wang M, Liang S, Shakhathreh MA, James D, Nishiyama S, Yoshimura F, Demuth DR (2008) Subversion of innate immunity by periodontopathic bacteria via exploitation of complement receptor-3. *Adv Exp Med Biol* 632, 203–19. [PubMed: 19025124]
92. Le Cabec V, Carréno S, Moisan A, Bordier C, Maridonneau-Parini I (2002) Complement Receptor 3 (CD11b/CD18) Mediates Type I and Type II Phagocytosis During Nonopsonic and Opsonic Phagocytosis, Respectively. *J Immunol* 169, 2003–9. [PubMed: 12165526]
93. Le Cabec V, Cols C, Maridonneau-Parini I (2000) Nonopsonic Phagocytosis of Zymosan and *Mycobacterium kansasii* by CR3 (CD11b/CD18) Involves Distinct Molecular Determinants and

- Is or Is Not Coupled with NADPH Oxidase Activation. *Infect Immun* 68, 4736–45. [PubMed: 10899880]
94. Xu S, Cooper A, Sturgill-Koszycki S, van Heyningen T, Chatterjee D, Orme I, Allen P, Russell DG (1994) Intracellular trafficking in *Mycobacterium tuberculosis* and *Mycobacterium avium*-infected macrophages. *J Immunol* 153, 2568–78. [PubMed: 8077667]
 95. Armstrong JA and Hart PD (1971) Response of cultured macrophages to *Mycobacterium tuberculosis*, with observations on fusion of lysosomes with phagosomes. *J Exp Med* 134, 713–40. [PubMed: 15776571]
 96. Malik ZA, Iyer SS, Kusner DJ (2001) *Mycobacterium tuberculosis* phagosomes exhibit altered calmodulin-dependent signal transduction: contribution to inhibition of phagosome-lysosome fusion and intracellular survival in human macrophages. *J Immunol* 166, 3392–401. [PubMed: 11207296]
 97. Mosser DM and Edelson PJ (1987) The third component of complement (C3) is responsible for the intracellular survival of *Leishmania major*. *Nature* 327, 329–31. [PubMed: 3035377]
 98. Mollinedo F, Janssen H, de la Iglesia-Vicente J, Villa-Pulgarin JA, Calafat J (2010) Selective fusion of azurophilic granules with *Leishmania*-containing phagosomes in human neutrophils. *J Biol Chem* 285, 34528–36. [PubMed: 20801889]
 99. Hoang KV, Rajaram MVS, Curry HM, Gavrilin MA, Wewers MD, Schlesinger LS (2018) Complement Receptor 3-Mediated Inhibition of Inflammasome Priming by Ras GTPase-Activating Protein During *Francisella tularensis* Phagocytosis by Human Mononuclear Phagocytes. *Front Immunol* 9, 561. [PubMed: 29632532]
 100. Bonsignore P, Kuiper JWP, Adrian J, Goob G, Hauck CR (2019) CEACAM3-A Prim(at)e Invention for Opsonin-Independent Phagocytosis of Bacteria. *Front Immunol* 10, 3160. [PubMed: 32117212]
 101. Tone K, Stappers MHT, Willment JA, Brown GD (2019) C-type lectin receptors of the Dectin-1 cluster: Physiological roles and involvement in disease. *Eur J Immunol* 49, 2127–33. [PubMed: 31580478]

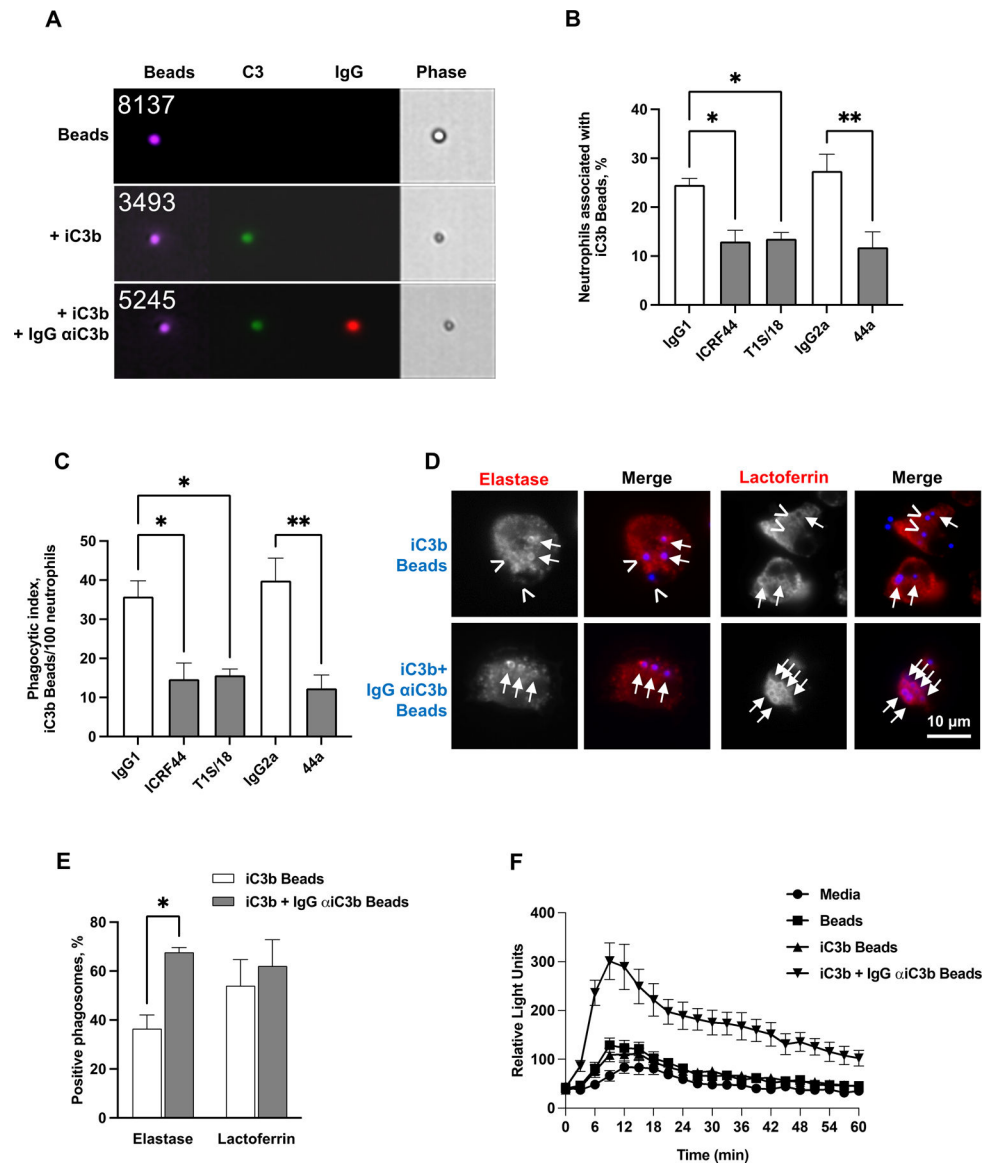


Figure 1. iC3b-coated beads are phagocytosed by neutrophils, but do not stimulate the oxidative burst or full phagosome maturation.

(A) Brilliant Blue™ polystyrene beads (purple) were left unopsonized (Beads), opsonized with human iC3b (iC3b beads), or opsonized with iC3b followed by 3E7 monoclonal antibody against human iC3b (iC3b + IgG α iC3b beads). Beads were stained with FITC-coupled antibody against human C3 (green) and Alexa Fluor 647-coupled antibody against mouse IgG (red). Representative images from imaging flow cytometry of unopsonized beads (top panel), iC3b-opsonized beads (middle panel), and iC3b-anti-iC3b opsonized beads (lower panel) are presented. The number of the particle in the population that was analyzed is presented on the top left of each bead image. (B-C) Adherent, PMA-treated primary human neutrophils were exposed to anti-CR3 blocking antibodies (anti-CD11b: ICRF44, 44a; anti-CD18: TS1/18; gray bars) or matched isotype control (white bars), then incubated with Bright Blue™ polystyrene beads opsonized with purified iC3b for 10 min. (B) The percent of neutrophils associated with iC3b-opsonized beads was determined by

imaging flow cytometry. **(C)** Neutrophils were fixed and processed for immunofluorescence microscopy. The number of phagocytosed iC3b-opsonized beads per 100 neutrophils was determined. For **(B-C)**, data are the mean \pm SEM for 3 biological replicates. Statistical significance was determined by ordinary one-way ANOVA with Sidak's multiple comparisons test. **(D-E)** Adherent, PMA-treated primary human neutrophils were exposed to beads (blue) opsonized with purified iC3b (iC3b) or purified iC3b followed by the 3E7 IgG monoclonal antibody against iC3b (iC3b + IgG α iC3b) for 30 min. Cells were fixed, permeabilized, and stained with an antibody against the primary granule protein neutrophil elastase or the secondary granule protein lactoferrin (red). The red channel is shown in grayscale to better show rings of staining surrounding positive phagosomes (arrows), or their absence around negative phagosomes (arrowheads), alongside the merged images. **(D)** shows representative images. **(E)** The percent of neutrophil elastase- and lactoferrin-positive phagosomes was quantified from over 100 cells from each of 3 biological replicates and presented as the mean \pm SEM. Statistical significance was determined by Student's paired *t* test. **(F)** Primary human neutrophils were left uninfected (media) or exposed to beads treated with iC3b, iC3b + IgG α iC3b, or untreated. ROS production was measured by luminol-dependent chemiluminescence as the relative light units (RLU) detected at each time point. The graph shown is from one representative experiment of four biological replicates, with three technical replicates per condition. *, *P* 0.05; **, *P* 0.01 for indicated statistical tests.

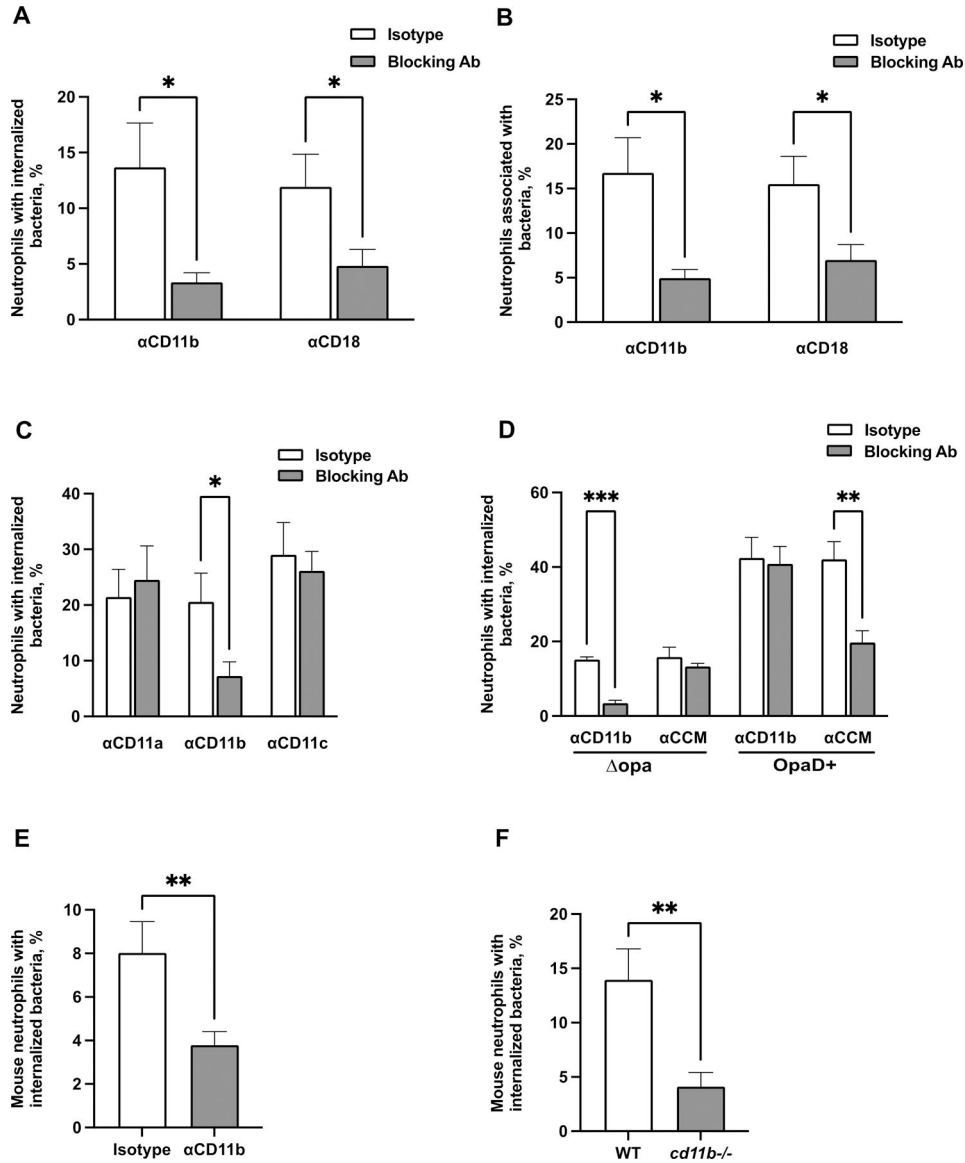


Figure 2. CR3-dependent phagocytosis of Opa-negative *N. gonorrhoeae* by adherent neutrophils. (A-B) Adherent, IL-8 treated primary human neutrophils were exposed to blocking antibodies against CD11b (44a) or CD18 (TS1/18) (gray bars), or matched isotype control (white bars). Neutrophils were infected with CFSE-labeled Δ opa Ngo for 1 hr, fixed, and stained for extracellular Ngo using a DyLight™ 650 (DL650)-labeled antibody without permeabilization. A step gate was applied to quantify the percentage of neutrophils with internalized (A) and associated (bound and internalized) (B) Ngo. (C) Neutrophils were treated with blocking antibodies against CD11a, CD11b, or CD11c, or isotype control. Internalization of Δ opa Ngo was measured as above. (D) Neutrophils were treated with blocking antibodies against human CEACAMs (CCM) or CD11b (44a). Internalization of Δ opa or OpaD+ Ngo was measured as above. (E-F) Neutrophils were purified from the bone marrow of WT or *cd11b*^{-/-} C57BL/6J mice. In E, adherent neutrophils from WT mice were exposed to anti-CD11b blocking antibody (M170) or isotype control. Neutrophils

were incubated with Tag-IT Violet[®] labeled *opa* Ngo for 1 hr, fixed, and stained for extracellular bacteria with DL650-labeled anti-Ngo antibody and for the neutrophil surface with FITC-coupled antibody against Ly6G. Cells were analyzed by imaging flow cytometry as above (see Fig. S5A for mouse neutrophil gating strategy), and the percent of mouse neutrophils with intracellular bacteria was calculated. Results presented are the mean \pm SEM of the following number of biological replicates: (A-B) 4–5; (C), 3–4; (D), 4; (E-F), 6. In **A-F**, statistical significance was determined by Student's paired *t* test. *, *P* 0.05, ***P* 0.01, *** *P* 0.001, **** *P* 0.0001.

Author Manuscript

Author Manuscript

Author Manuscript

Author Manuscript

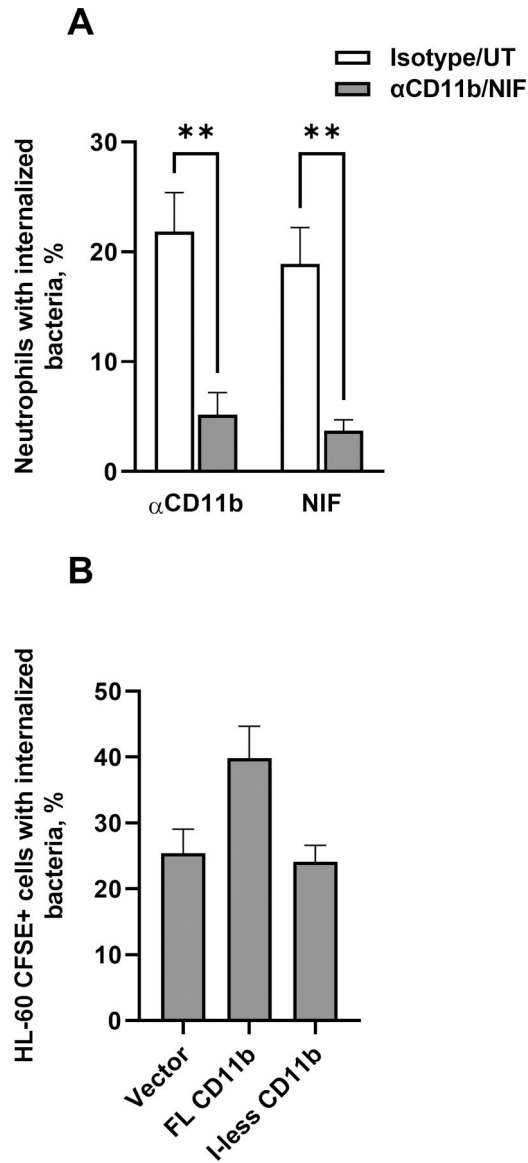


Figure 3. The I-domain and MIDAS motif of CD11b are critical for CR3-mediated phagocytosis of Opa-negative *N. gonorrhoeae*.

(A) Adherent, IL-8 treated primary human neutrophils were treated with (left group) anti-CD11b (44a; gray bar) or isotype control (white bar), or (right group) *A. caninum* neutrophil inhibitory factor (NIF) (gray bar) or PBS vehicle control (white bar; UT = untreated). The percent of neutrophils with intracellular Ngo was calculated using imaging flow cytometry as in Fig. 2. Results are presented as the mean \pm SEM for 3 biological replicates, with statistical significance determined by Student's *t* test for the appropriate pairs. ** *P* 0.01. (B) HL-60 human promyelocytic cells expressing human CD11b that is full-length (FL) or lacking the I-domain (I-less), or carrying empty vector (Vector), were exposed to CFSE-labeled opa Ngo for 1 hr. Cells were fixed, stained for extracellular Ngo, and processed for imaging flow cytometry. The percent of CFSE+ HL-60 cells with intracellular Ngo was calculated for 3 biological replicates. Results are presented as the mean \pm SEM.

Comparisons trended towards but did not reach statistical significance as analyzed using one-way ANOVA.

Author Manuscript

Author Manuscript

Author Manuscript

Author Manuscript

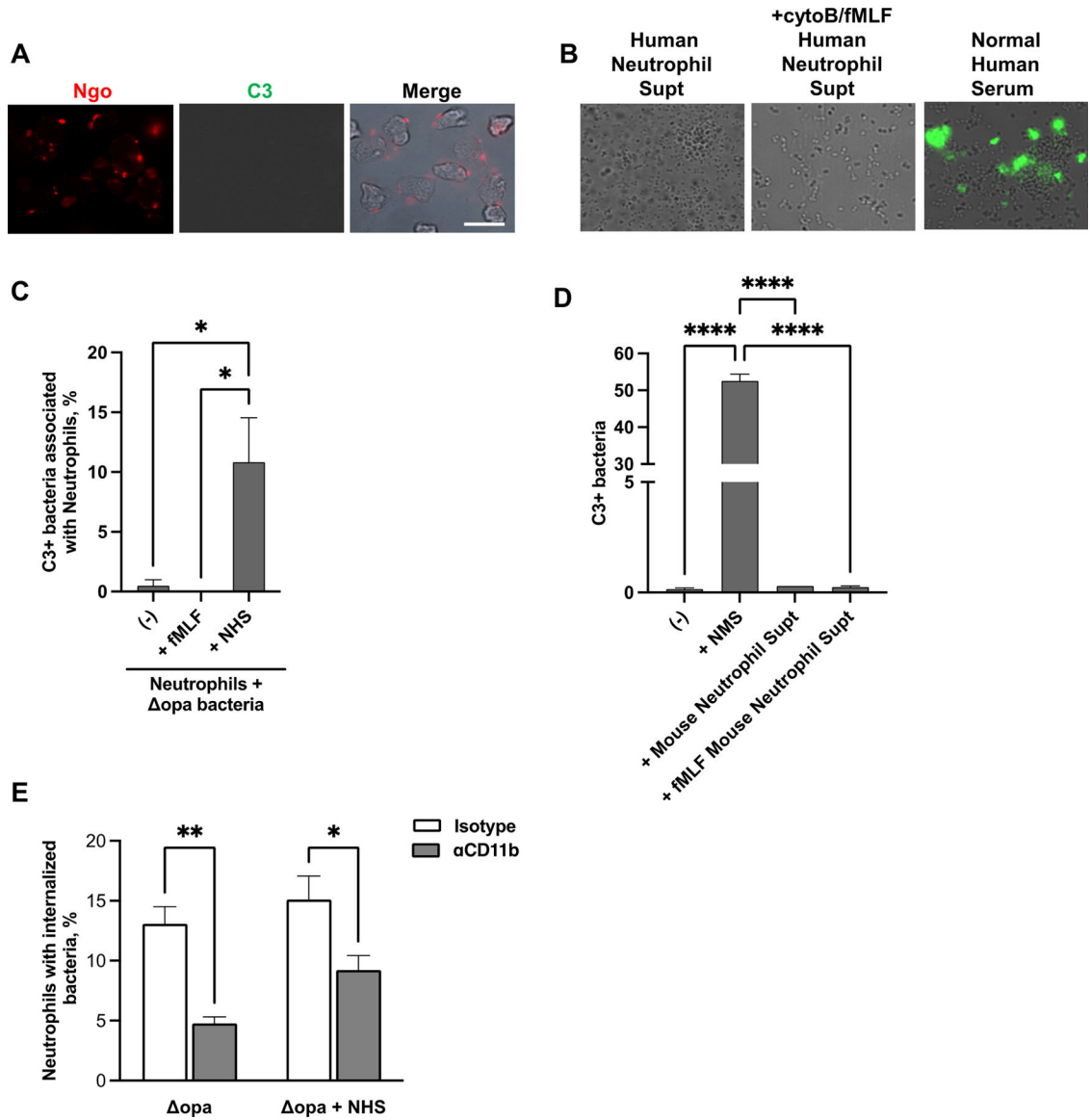


Fig. 4. Human neutrophils are not a source of C3 for opsonization of *N. gonorrhoeae*.

(A) Adherent, IL-8 treated primary human neutrophils were exposed to non-opsonized opa Ngo for 15 min, fixed, and stained with FITC-labeled anti-C3 (green) and DL650-labeled anti-Ngo (red) antibodies. Fluorescence micrographs were captured for the FITC and DL650 channels (presented as grayscale), with the merge in color showing overlap with the phase image for the neutrophils. (B) opa Ngo was incubated with normal human serum as a positive control for C3 opsonization (third panel), or with the supernatants collected from adherent primary human neutrophils that were left untreated (first panel) or treated with cytochalasin B (cytoB) and fMLF to stimulate degranulation (second panel). Bacteria were washed and stained with FITC-labeled anti-C3 antibody. Representative fluorescence micrographs with the FITC channel overlaid on the phase image are presented. (C) Neutrophils were treated with cytoB + fMLF as above, or left untreated (-). Neutrophils were exposed for 15 min to unopsonized opa Ngo. Neutrophils were fixed, stained with

FITC-labeled anti-C3 antibody and DL650-labeled anti-Ngo antibodies, and analyzed by imaging flow cytometry. The spot count feature was used to quantify cells with positive FITC signals within the population of neutrophils containing 1–3 DL650+ Ngo for 3 biological replicates. Untreated neutrophils exposed to opa Ngo that was opsonized in normal human serum (ops) served as a positive control. **(D)** opa Ngo was left untreated, or incubated with the supernatant from adherent mouse neutrophils that were untreated (Mouse Neutrophil Supt) or treated with cytoB + fMLF (+fMLF Mouse Neutrophil Supt). Ngo was incubated with 50% normal mouse serum as a positive control (+NMS) or PBS as a negative control (-). Ngo was washed and stained with FITC-labeled anti-mouse C3 antibody and analyzed by imaging flow cytometry as in **C**. The percent of bacteria that were in the C3+ gate was quantified from 3 biological replicates. **(E)** Adherent, IL-8 treated primary human neutrophils were exposed to anti-CD11b (44a; gray bars) or isotype control (white bars), then infected with opa Ngo that was not opsonized (left) or opsonized in normal human serum as in **B** (right). The percent of neutrophils with internalized Ngo was quantified by imaging flow cytometry as in Fig. 2. Results presented are for 4–6 biological replicates. Statistical significance in **C-D** was determined by ordinary one-way ANOVA with Tukey's multiple comparisons test, and in **E** by paired Student's *t* test. * $P < 0.05$, ** $P < 0.01$ ***, $P < 0.001$, **** $P < 0.0001$.

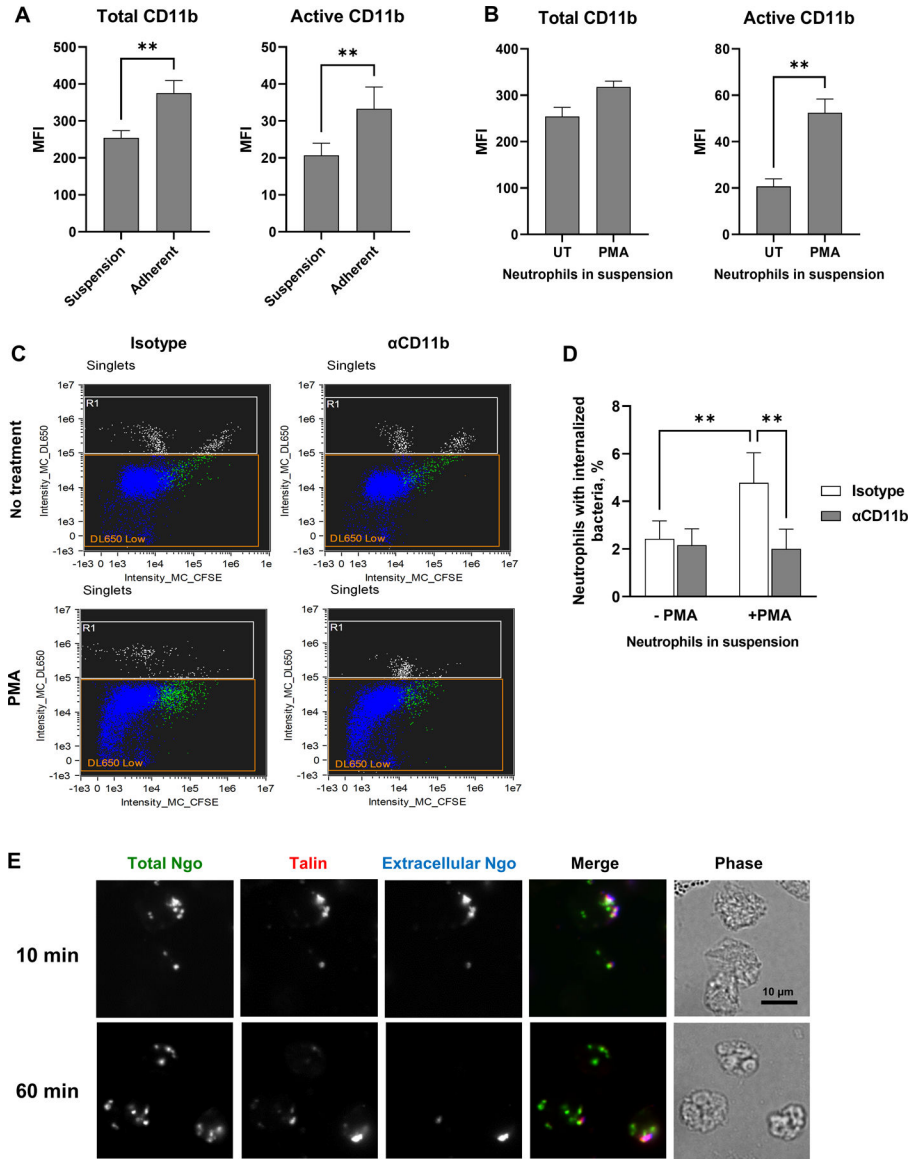


Figure 5. Active CR3 promotes phagocytosis of Opa-negative *N. gonorrhoeae* by human neutrophils in suspension.

(A) Human neutrophils were maintained in suspension or allowed to adhere to coverslips in the presence of IL-8. The median fluorescence intensity (MFI) of total (left) and active (right) CD11b on the neutrophil surface from $n = 5$ biological replicates is presented. (B) Neutrophils in suspension were left untreated (UT) or treated with PMA, then stained for total (ICRF44; left) and active (CBRM1/5; right) CD11b. The MFI from $n = 5$ biological replicates is presented. (C-D) Untreated or PMA-treated neutrophils in suspension were exposed to anti-CD11b antibody or isotype control, then infected with CFSE-labeled opa Ngo at MOI = 1. Phagocytosis was measured by imaging flow cytometry as in Fig. 2. (C) Dot plots of the intensity of CFSE (total Ngo) vs. intensity of DL650 (extracellular Ngo). Intact, single neutrophils are identified as the DL650 Low population (blue; R1 = gate for DL650^{hi} cells that are not intact). The green color identifies the population of neutrophils that are associated with CFSE+ Ngo. (D) The percentages of untreated and PMA-treated

neutrophils with internalized bacteria were calculated. Results presented are the mean \pm SEM from n=4 biological replicates. **(E)** Adherent, IL-8 treated human neutrophils were exposed to CFSE+ opa Ngo (green) for 10 min to allow for attachment, or 60 min to allow for internalization. Cells were fixed, stained for extracellular Ngo (blue), then permeabilized and stained for talin (red). Colocalization between extracellular, cell-associated Ngo and talin is seen in the 10 min merged image. Statistical significance was determined by paired Student's *t* test (**A-B**) or two-way ANOVA followed by Sidak's multiple comparison test (**D**) for 5 biological replicates. ** *P* < 0.01.

Author Manuscript

Author Manuscript

Author Manuscript

Author Manuscript

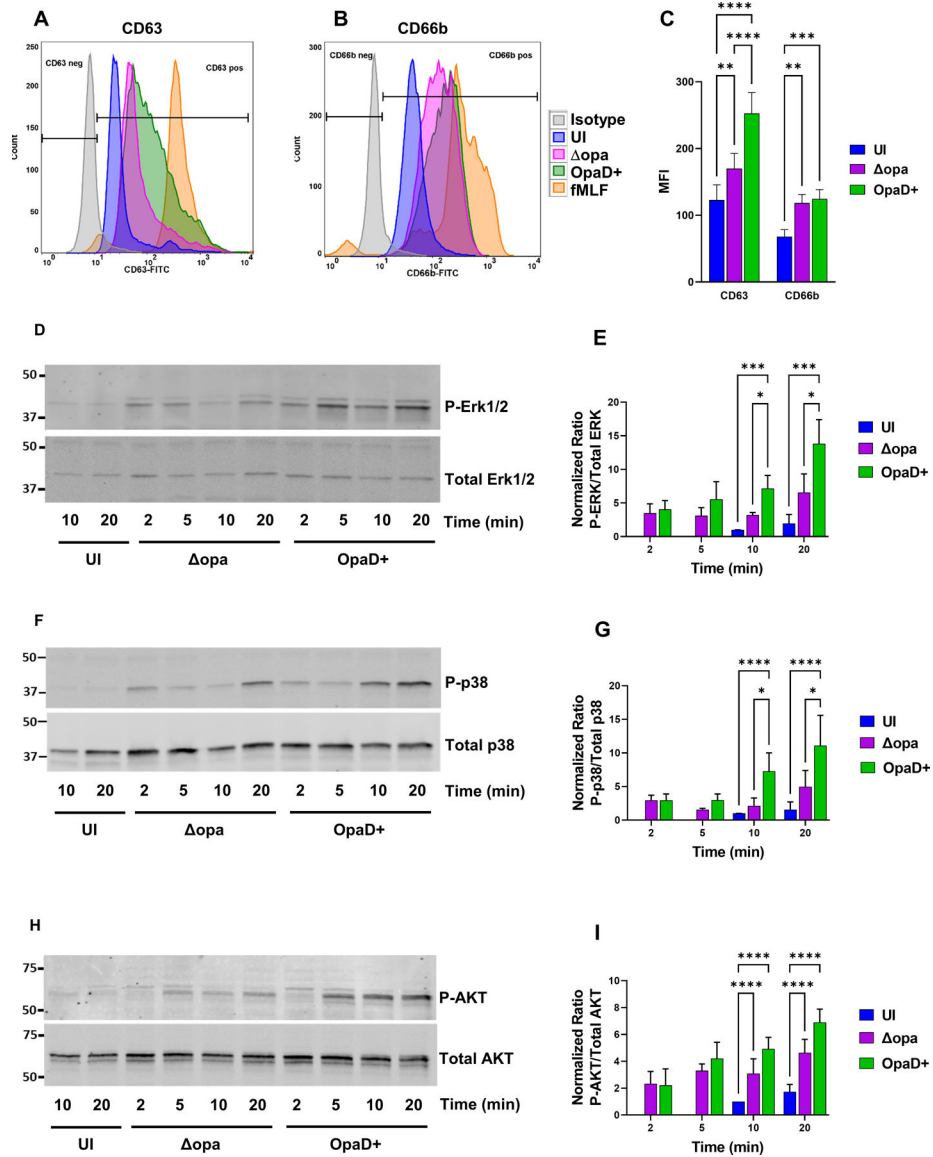


Figure 6. Limited activation of neutrophils following exposure to Opa-negative *N. gonorrhoeae*. (A-C) Adherent, interleukin 8-treated primary human neutrophils were exposed to *opa* or OpaD+ Ngo for 1 hr, or left uninfected (UI). Surface presentation of CD63 (primary granules) (A) and CD66b (secondary granules) (B) was measured by flow cytometry. Neutrophils treated with cytochalasin B + fMLF served as a positive control for degranulation (fMLF). The geometric mean fluorescence intensity (MFI) \pm SEM was calculated from $n = 6$ biological replicates (C), with statistical significance determined by two-way ANOVA with Sidak's multiple comparisons test. (D-I) Adherent, IL-8 treated neutrophils were incubated with *opa* or OpaD+ Ngo or left uninfected for the indicated times (UI). Whole cell lysates were immunoblotted for phosphorylated and total p38, ERK1/2, and AKT. D, F, and H show a representative blot from one of three biological replicates. E, G, and I report the ratio of phosphorylated to total protein by quantitative immunoblot for the three replicates, relative to the uninfected condition at 10 min (whose

ratio set to 1). Statistical significance was determined by two-way ANOVA followed by Tukey's multiple comparisons test for 3 (**G**) or 4 (**E, I**) biological replicates. * $P < 0.05$, ** $P < 0.01$, *** $P < 0.001$, **** $P < 0.0001$.

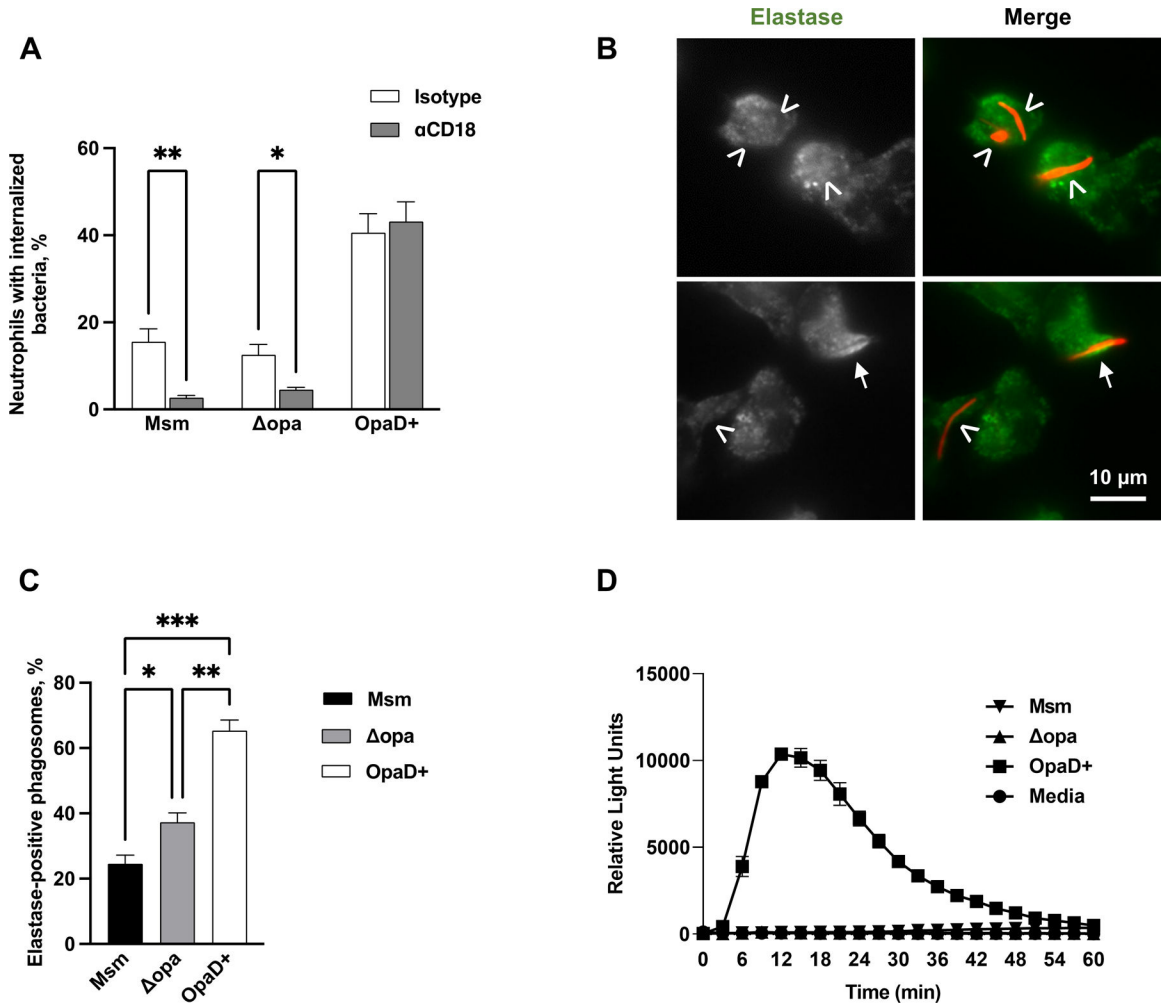


Figure 7. Phagocytosis of *M. smegmatis* by human neutrophils is CR3-dependent and does not stimulate the oxidative burst or full phagosome maturation.

(A) Adherent, IL-8 treated human neutrophils were treated with either isotype control or anti-CD18 antibody, then exposed to Tag-IT Violet™ labeled *M. smegmatis* (Msm) for 1 hr. Neutrophils were fixed, stained for CD11b, and examined by imaging flow cytometry. Intracellular bacteria were defined as those within a mask set by the CD11b surface staining eroded by 4 pixels and quantified by spot count (see Fig. S9). The percent of neutrophils with intracellular *M. smegmatis*, Δ opa Ngo, and OpaD+ Ngo, with and without CD18 blockade, was calculated from 5 biological replicates and presented as the mean \pm SEM. (B-C) Adherent, IL-8 treated human neutrophils were infected with mCherry-expressing *M. smegmatis* at MOI = 5 for 1 hr (red). Cells were fixed, permeabilized and stained for neutrophil elastase (green). Two representative panels with neutrophils and *M. smegmatis* are shown in (B), with the grayscale elastase signal on the left and merged fluorescence image with *M. smegmatis* on the right. The arrows identify elastase-positive phagosomes; arrowheads, elastase-negative phagosomes. The percent of elastase-positive phagosomes containing *M. smegmatis*, Δ opa Ngo, and OpaD+ Ngo was quantified from 50–100 phagosomes per condition. Results presented are the mean \pm SEM from 4 biological replicates. (D) Primary human neutrophils were left uninfected (media) or exposed to *M.*

smegmatis, or opa or OpaD+ Ngo at MOI = 100. ROS production by luminol-dependent chemiluminescence was measured as in Fig. 1E. The graph shown is from one representative of 3 biological replicates. Each data point is the mean \pm SEM from three technical replicates. Statistical significance was determined by statistical Student's paired *t* test (A) or repeated measures one-way ANOVA followed by Tukey's multiple comparisons test (C). * *P* 0.05, ** *P* 0.01, *** *P* 0.001.

Author Manuscript

Author Manuscript

Author Manuscript

Author Manuscript

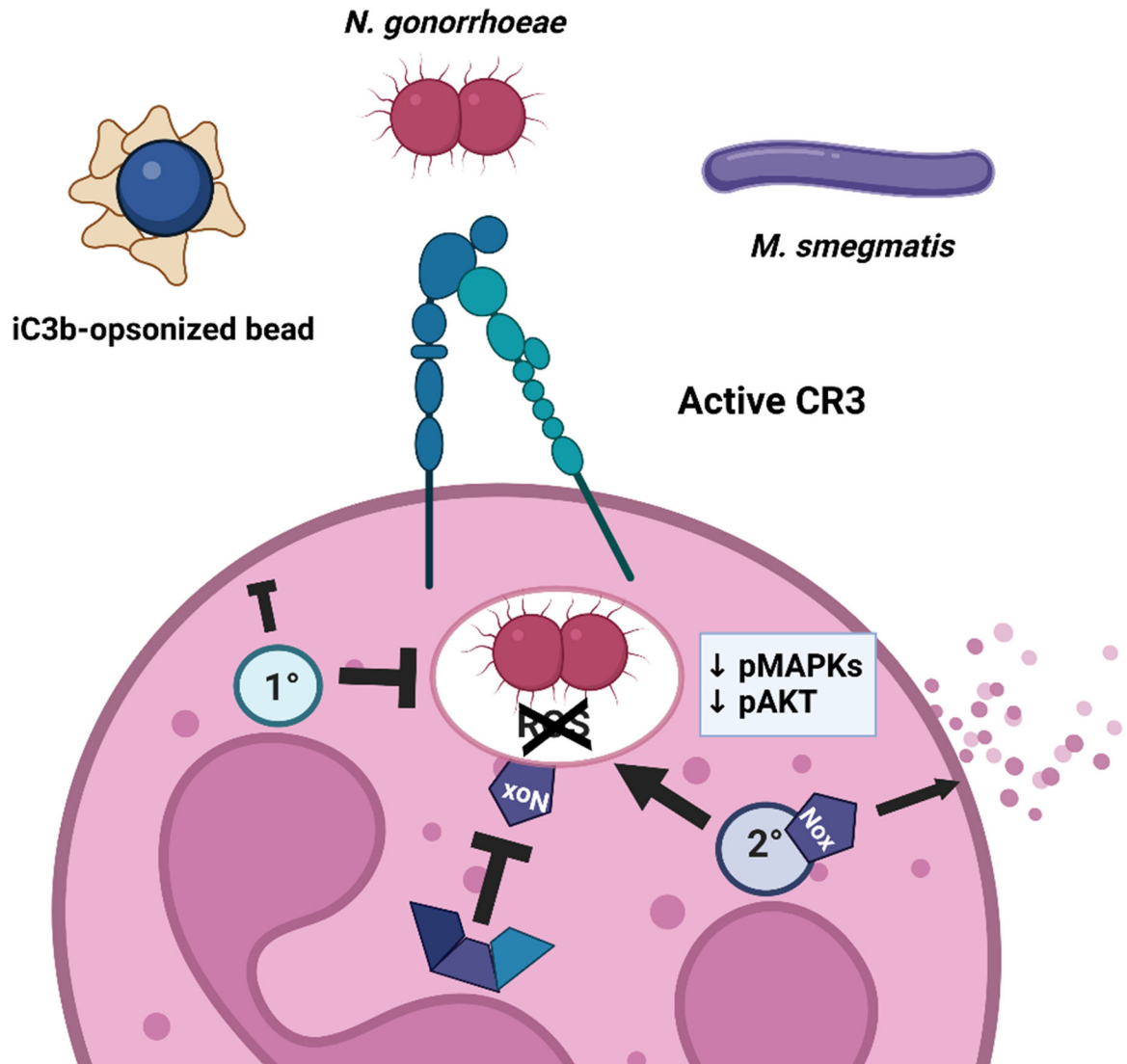


Figure 8.

CR3-mediated phagocytosis is a silent entry pathway into neutrophils.

Non-opsionized substrates that are phagocytosed into neutrophils via CR3 do not induce the oxidative burst, poorly activate inflammatory signaling cascades, and predominantly reside in immature phagosomes. While this pathway of silent entry would facilitate non-inflammatory clearance of iC3b-tagged apoptotic cells and immune complexes (recapitulated in this study by use of iC3b-coated polystyrene beads), it is exploited by diverse microbes, including *Neisseria gonorrhoeae* and *Mycobacterium smegmatis*, to avoid degradation and killing within neutrophils.

Table 1.

Antibodies used in this study.

Target	Antibody/Clone Name	Species, Isotype	Label	Source	Use	Comments
CD11b, human	44a	mouse IgG2a	(-)	E. Hewlett	Function Blocking	Purified at UVA Hybridoma Core; no azide
CD11b, human	ICRF44	mouse IgG1	(-)	Biolegend	Function Blocking	LEAF™ Purified
CD11b, human	ICRF44	mouse IgG1	PE	eBiosciences	Flow cytometry	Reports total surface CD11b
CD11b, human and mouse	M170	rat IgG2b, κ	(-)	E. Hewlett	Function Blocking	Purified at UVA Hybridoma Core; no azide
CD11b, human and mouse	M170	rat IgG2b, κ	PE	Biolegend	Flow cytometry	
CD11b, active, human	CBRM1/5	mouse IgG1	APC	Biolegend	Flow cytometry	Reports active conformation of CD11b
CD18, human	TS1/18	mouse IgG1, κ	(-)	Thermo Fisher Scientific	Function Blocking	LEAF™ Purified
CD11a, human	HI111	mouse IgG1, κ	(-)	Biolegend	Function Blocking	LEAF™ Purified
CD11c, human	Clone 3.9	mouse IgG1, κ	(-)	Biolegend	Function Blocking	LEAF™ Purified
C3, human	Anti-human C3	goat	FITC	MP Bio/Cappel	IF, Western blot	
C3b/iC3b, human	3E7	mouse IgG1	(-)	R. Taylor	Function Blocking, Flow Cytometry	Purified at UVA Hybridoma Core
N. gonorrhoeae		rabbit	(-)	Meridian	Flow cytometry, IF	Labeled in-house with DyLight 650, Alexa Fluor 555, or Alexa Fluor 647
Opa proteins	4B12	mouse IgG2a	(-)	Criss lab stock	Western blot	Purified at UVA Hybridoma Core
CD63, human	AHN16.1	mouse	FITC	Ancell	Flow cytometry	
CD66b, human	CLB-B13.9	mouse	FITC	Sanquin Peliclusier	Flow cytometry	
CD14, human	MΦP9	mouse IgG2b	BV711	Becton Dickinson	Flow cytometry	For neutrophil purity
CD49d, human	9F10	mouse IgG1, k	PE	Biolegend	Flow cytometry	For neutrophil purity
CD16, human	3G8	mouse IgG1, k	BV421	Biolegend	Flow cytometry	For neutrophil purity
CEACAMs, human	D14HD11	mouse IgG1	(-)	Origene	Function Blocking	
Ly6G, mouse	1A8	rat IgG2a, κ	FITC	Biolegend	Flow cytometry	
Lactoferrin, human		rabbit	(-)	MP Bio/Cappel	IF	
Neutrophil elastase, human	AHN10	mouse IgG1, κ	(-)	Sigma-Aldrich	IF	Labeled in-house with AF555 (Thermo Fisher)

Target	Antibody/Clone Name	Species, Isotype	Label	Source	Use	Comments
Talin, human	8D4	mouse IgG1	(-)	Sigma-Aldrich	IF	Labeled in-house with AF555 (Thermo Fisher)
IgG, rabbit		goat	AF555	Thermo Fisher Scientific	IF	Highly cross-absorbed
IgG, rabbit		goat	AF488	Thermo Fisher Scientific	IF	Highly cross-absorbed
IgG, mouse		goat	AF488	Thermo Fisher Scientific	IF	Highly cross-absorbed
IgG, mouse		goat	AF647	Thermo Fisher Scientific	IF	Highly cross-absorbed
Isotype control	MOPC-21	mouse IgG1	FITC	eBiosciences	Flow cytometry	
Isotype control	MOPC-21	mouse IgG1	APC	Biolegend	Flow cytometry	
Isotype control	P3.6.2.8.1	mouse IgG1	PE	eBiosciences	Flow cytometry	
Isotype control	15H6	mouse IgG1	(-)	Southern Biotech	Function Blocking	
Isotype control	HOPC-1	mouse IgG2a	(-)	Southern Biotech	Function Blocking	
Isotype control	RTK4530	rat IgG2b, κ	PE	Biolegend	Flow cytometry	
Akt, human	E7J2C	mouse	(-)	Cell Signaling	Western blot	
Phospho-Akt (Thr308)	C31E5E	rabbit mAb	(-)	Cell Signaling	Western blot	
Erk1/2, human	3A7	mouse mAb	(-)	Cell Signaling	Western blot	
phospho-Erk 1/2 (MAPK Thr202/Tyr204)	9101	rabbit mAb	(-)	Cell Signaling	Western blot	
p38, human	9212	rabbit mAb	(-)	Cell Signaling	Western blot	
phospho-p38 (Thr180/Tyr182)	28B10	mouse mAb	(-)	Cell Signaling	Western blot	
Mouse IgG (H+L)		goat	DyLight 800	Thermo Fisher Scientific	Western blot	
Rabbit IgG (H+L)		goat	AF680	Thermo Fisher Scientific	Western blot	